UNIVERSITY OF CALIFORNIA, MERCED

Solar Thermal Powered Evaporators

A Thesis submitted in partial satisfaction of the requirements
for the degree of Master of Science

in

Mechanical Engineering and Applied Mechanics

by

Christian Robert Moe

Committee in charge:

Professor Gerardo Diaz
Professor Jian-Qiao Sun
Professor Roland Winston

2014

The Thesis of Christian Robert Moe is approved, and it is acceptable in quality and form for publication on microfilm and electronically:

Professor Roland Winston, Advisor and Committee Member

Professor Jian-Qiao Sun, Committee Member

Professor Gerardo Diaz, Committee Chair

University of California, Merced

2015

Table of Contents

List of Figures

Abstract

Solar Aided Desalination

Christian Robert Moe

Mechanical Engineering and Applied Mechanics

University of California, Merced 2014

Committee Chair: Gerardo Diaz

Access to potable water is necessary for human development. Industry, farms, and the public all need clean sources of water. Generally this water is available locally through natural sources such as rivers or wells, but there are many cases where additional clean water is needed. This includes desert regions and cities that have outgrown their natural water sources.

California, where some cities are outgrowing their water supply, is currently facing a multi-year drought. California already has several desalination plants, with the first major utility scale plant being installed near San Diego [1]. However, few responses have been made toward inland areas, such as the vast farming region of the California Central Valley.

The once vast underground water reserves of the California Central Valley are drying up. Land in some regions has subsided as much as 25 feet due to aquifer use [2]. California agriculture makes up one sixth of the total irrigated land in the United States, making the region too important to ignore.

The ongoing water scarcity in California is a problem of enormous scale, with the farms and food processing industries being good candidates for wastewater reuse. According to the California Department of Water Resources, the collective agricultural industry uses around 80% of the fresh water in the state [3]. This leads to two large sources of wastewater, farm runoff and agricultural processing waste streams. To help the agricultural industry continue, water streams could be used more effectively and many waste streams could be recovered.

Desalination systems have the potential to take most wastewater streams and generate useful water. If the agricultural wastewater streams were reused, it could lower the overall water needs and increase water security for the California Central Valley.

An abundant resource in California that could be utilized to aid in this task is solar energy. Solar thermal collector arrays can be used for pre-heating to reduce electricity costs in a reverse osmosis system or be used as the driving energy in a distillation system.

This thesis touches on the major desalination systems currently in use, including components that can be aided or powered by solar thermal energy. A section is also devoted to cover the basic process of zero liquid discharge, which removes the waste stream from desalination installations. Finally, this thesis goes in depth into a project to augment a current solar thermal loop and demonstrate solar thermal technology being used with an evaporator.

1 Introduction

This thesis focuses on the desalination systems for generating useful water from wastewater streams of different salt concentrations. It focuses mostly on utilizing waste streams from farm runoff. This thesis also touches on integrating solar thermal collectors with desalination processes, including simulating a demo project to demonstrate solar thermal systems with an evaporator.

It is important to note what category of water is treatable through desalination and what category is useful. The different categories of water types are potable, graywater, and blackwater. Potable is used to define water fit for human consumption and food preparation. Graywater is lightly dirtied water, such as runoff from sinks and showers. Runoff from farms and food processing plants will be included in the graywater category as well. The blackwater category is reserved for water that has significant biological wastes and is not a good candidate for reuse.

Graywater streams are generally higher in salt levels and has limited use unless the salt is removed. Desalination systems produce fresh water at the cost of energy and produce a concentrated brine holding the remaining salts. Large streams of graywater with fairly steady salt contents are usually good candidates for desalination systems. Different desalination technologies handle different concentrations of salt. With the correct desalination selection, as much as 90% of the incoming water can be recovered [4].

The resulting water product from a desalination plant is often pure enough to be potable, but may not recommended for human used due to the source of the feed water. The best use for the product water is the system that generated the feed water as a byproduct. For example, if a farm or plant generates a lot of waste water they will likely have high water needs. If a majority of the water is recovered and fed back to the farm or plant it would demand much less water from other sources.

In addition to creating product water, all desalination systems also create a highly concentrated salt brine. To dispose of this brine, evaporators can be installed to concentrate the water until dry salts can be harvested with a filter press. The salts can then be inexpensively disposed of or sold. The process of eliminating all liquid disposals from a desalination plant is call zero liquid discharge.

1.1 Desalination Overview

Every desalination system takes in salt water and generates two streams. One stream is pure water, often defined as the product or percolate. The other stream is concentrated salt water, usually referred to as brine.

Desalination systems generally fall into two broad categories. Osmotic systems push against the osmotic pressure of the brine to make its product, while distillation systems evaporate nearly pure water from the brine.

The brine generated from a desalination system is considered a waste stream, unless the salt can be removed as a dry product. The process of generating dry salts from the waste stream is discussed later in the zero liquid discharge section.

1.1.1 Defining the Work Done

The salt water has an osmotic pressure, which must be overcome in any desalination process to generate pure water. This osmotic pressure can be calculated if the salt concentration and type of salts are known in the salt water stream [5]. The equation to find the osmotic pressure is shown below [6].

$$\Pi = iMRT \qquad i \approx 1 \qquad R = 8.31\left(\frac{L\ k\text{Pa}}{K\ \text{mol}}\right) \tag{1}$$

To give an example, ocean water has a Total Dissolved Solids (TDS) count of 36000 parts per million (ppm). It is assumed that the dissolved solids are mostly sodium and chlorine ions. 36000 ppm can be converted directly into 36000 mg per liter, because water at any salt concentration has an approximate density of 1.0 kg per liter. Using this average atomic weight, the osmotic pressure can be found.

$$M = \frac{\left(36000\frac{mg}{L}\right)}{\left(29.225\frac{g}{\text{mol}}\right)} = 1.232\frac{\text{mol}}{L} \tag{2}$$

$$\Pi = (1)(1.232)(8.31)(290)M\text{Pa} = 3.0M\text{Pa} \tag{3}$$

This result gives an approximate osmotic pressure of 3.0 MPa, which is fairly close to the accepted solution of about 2.7 MPa for seawater at that salt concentration. The salt makeup is likely the main factor in the 10% discrepancy.

The work done can be defined as the osmotic pressure difference between brine and clear water multiplied by the volume of pure water generated. Using this definition of work, an estimate of the efficiency of the different desalination systems can be made if we know the energy requirements of each system. This definition can be applied regardless of the method used, as long as we assume nearly pure water as the product.

$$\text{Pa} \cdot m^3 = \frac{kg}{m\ s^2}\ m^3 = N \cdot m = J \tag{4}$$

For Engineers, it may sound like a good idea to call this work being done a change in the 'osmotic potential' between the feed water and pure water. However, that term has already been defined as a type of negative osmotic pressure, where pure water has a zero pressure and any change in osmotic pressure is a negative value. This was done to more easily explain how salt water can 'pull' fresh water through a membrane, as in define the pressure change as a 'potential' to move water. This definition does not conform to the idea of potentials in the engineering fields and should be noted to avoid future confusion.

By incorporating the density of water, we can convert between the osmotic pressure and the energy needed to generate pure water from the feed water. If an osmotic pressure of 1 MPa is used, the energy needed can be found with the equation below.

$$\rho_w = 1000\frac{kg}{m^3}, \qquad \Pi \cdot \rho_w = 1MPa \cdot 1000\frac{kg}{m^3} = 1\frac{kJ}{kg} \tag{5}$$

When pure water is removed from the feed water, the TDS of the remaining feed water increases. The above equations works if the amount of pure water generated is small in comparison to the feed water. In cases where a significant amount of pure water is removed from the feed, the salinity of the water will increase along with the energy needed to generate pure water.

The energy calculations need to be altered to account for the changing salt concentration. The instantaneous osmotic pressure as water is recovered can be estimated by the following equation.

$$\Pi = \Pi_0\left(\frac{1}{1-x}\right), \qquad x = \text{percent water recovered} \tag{6}$$

Where p_0 is the starting osmotic pressure of the feed water and x is the current percent that has been converted into pure water. Integrating this equation will result in the average osmotic pressure encountered during the desalination procedure.

$$\Pi_{\text{avg}} = \frac{\left(\int_0^{x_f} \Pi_0\left(\frac{1}{1-x}\right)dx\right)}{x_f} = \frac{\Pi_0\left(-\ln\left(1-x_f\right)\right)}{x_f} \tag{7}$$

This equation can now be used to find the energy required to remove significant percentages of fresh water from the feed water. For example, when removing 50% fresh water from sea water ($\text{TDS} = 36000\ \text{ppm},\ P_0 = 2.7\ M\text{Pa},\ x_f = 0.5$) it can be estimated that:

$$\frac{(2.7\ M\text{Pa})(-\ln(1-0.5))}{0.5} = 3.7\ M\text{Pa} \rightarrow 3.7\frac{kJ}{kg} \tag{8}$$

In this scenario, every kg of fresh water removed from sea water requires 3.5 kJ of energy per kilogram of fresh water generation.

1.2 Desalination Technologies

There are certain desalination systems that were selected for review based upon their prevalence and/or application alongside solar thermal systems. This includes a range of electrically and thermally driven systems. Desalination systems fall into two categories of osmotic and distillation technologies. Osmotic systems perform work directly against the osmotic pressure of the brine, while distillation systems evaporating pure steam out of the brine. Both technologies perform the same work, meaning the efficiencies can be directly compared.

1.2.1 Osmotic Technologies

1.2.1.1 Electrodialysis

Electrodialysis systems consist of 'electrodes' that pull the positive and negative salt ions away from the product streams. Their progress is halted in the concentrate streams by positively and negatively charged fluid membranes. The central stream(s) becomes more pure, while the side streams near the electrodes become brine.

This technology is best suited for low TDS applications where some salt is still desired in the product stream, such as drinking water [7]. This technology is not useful with high TDS water streams and is ineffective at producing water of high purity.

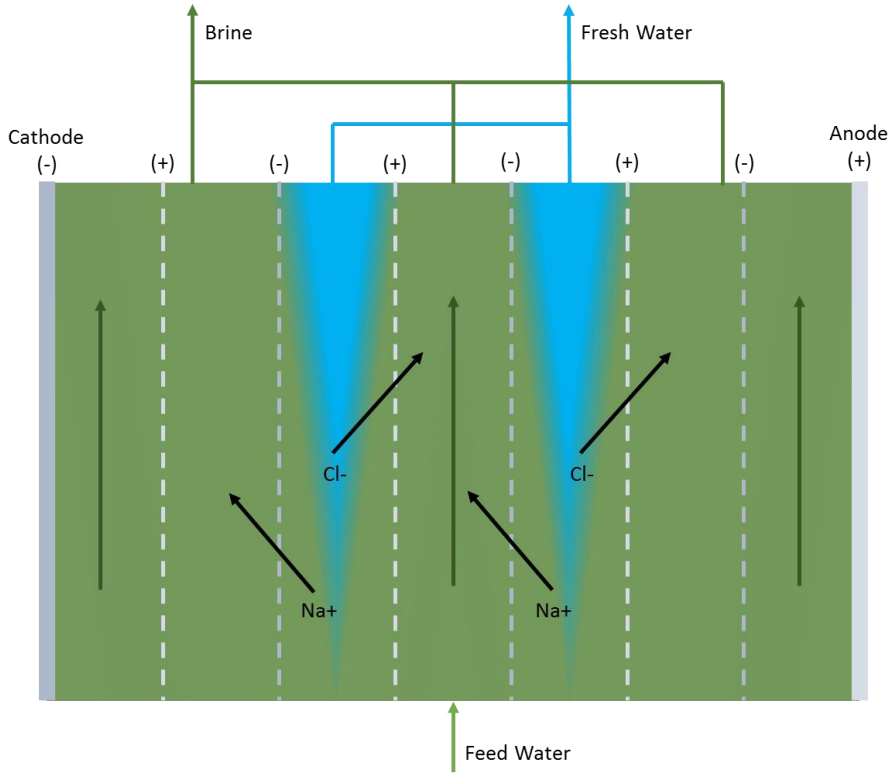

Figure 1: Electrodialysis diagram

1.2.1.2 Reverse Osmosis

Reverse Osmosis (RO) systems consists of a large pressure gradient that pushes water through a membrane. The membrane provides a barrier to the salts, allowing only clean water to pass through. The large pressure gradient overcomes the osmotic pressure of the brine, forcing water clean water to separate from the brine.

These systems can recover much of the pressure lost in the discharge stream through methods including pressure-pumps. Additionally, these systems run more efficiently and can handle slightly higher salt concentrations when the incoming water stream is warmed above ambient temperature [8]. This temperature has a maximum, based upon the membrane polymer, between 35 and 45 Celsius.

RO systems leave a small remnant of salt left in the fresh water stream. RO is a good technology to use with moderate amounts of salt in the feed water. To attain water pure enough to drink, some higher salinity feed water requires two stages of RO systems. For example, seawater often requires passing through two RO units before it is pure enough to drink.

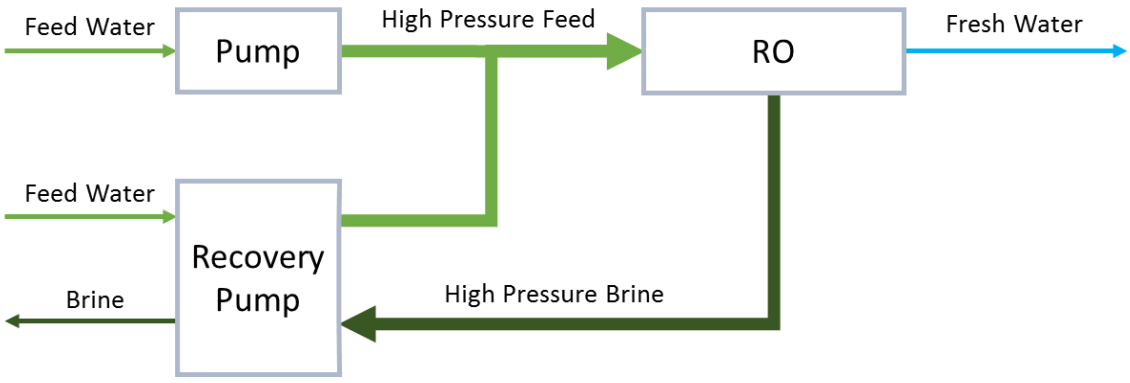

Figure 2: Reverse osmosis diagram

1.2.2 Distillation Technologies

Distillation systems covered include Multi-Stage Flash distillation (MSF), Multiple-Effect Distillation (MED), Multiple-Effect Membrane Distillation (MEMD), and Mechanical Vapor-Compression distillation (MVC) systems. Each one of these evaporates water in one chamber and condenses the pure water vapors as the water product. All the systems besides MVC require thermal energy as their primary energy source.

All of these systems leave extremely small amount of salt left in the produced fresh water. This may be desirable for lowering the salt concentration for soil, but for drinking purposes a small amount of salt needs to be added back to the fresh water.

1.2.2.1 Multi-Stage Flash

MSF systems heat the feed water up to 120 Celsius and moves the water from higher to lower pressure and temperature to 'flash' boil a portion of the water at each stage. The lowest pressures can be below ambient to drive additional evaporation, at the expense of running a vapor compression pump. The steam generally condenses on pipes cooled by the incoming water, which recovers most of the energy used in evaporation [9].

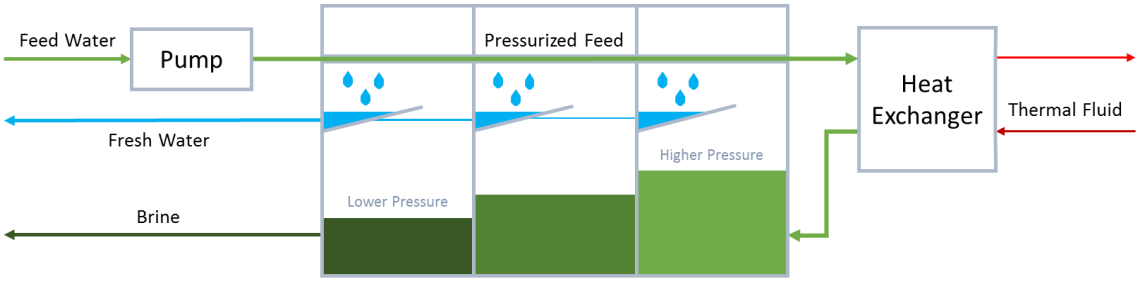

Figure 3: Multi-stage flash diagram

1.2.2.2 Multiple-Effect Distillation

MED systems heat the water below 100 Celsius. This process uses the temperature difference between the incoming water and heated water to drive evaporation from the warmed water to the condensing pipes. This also helps recover the energy used in evaporation. MED systems are typically large compared to the other desalination technologies, as they generally evaporate water at ambient pressure. This requires significantly more surface area to produce the same amount of distilled water compared to a technology that uses a pressure drop, such as MSF distillation.

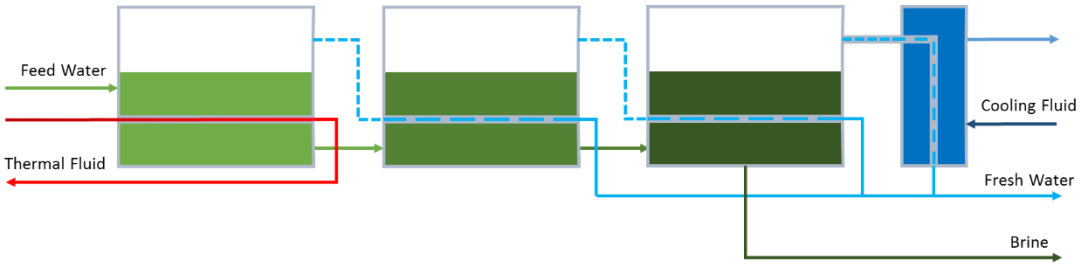

Figure 4: Multiple-effect distillation diagram

1.2.2.3 Multiple-Effect Membrane Distillation

MEMD systems are much like MED systems, but places a membrane between the evaporation and condensing areas. This has the benefit of being able to place the components very close together and becomes more space efficient, solving the size problems associated with MED systems. The membrane is generally made out of polypropylene, which can't handle the slightly higher temperatures common among MED systems [10].

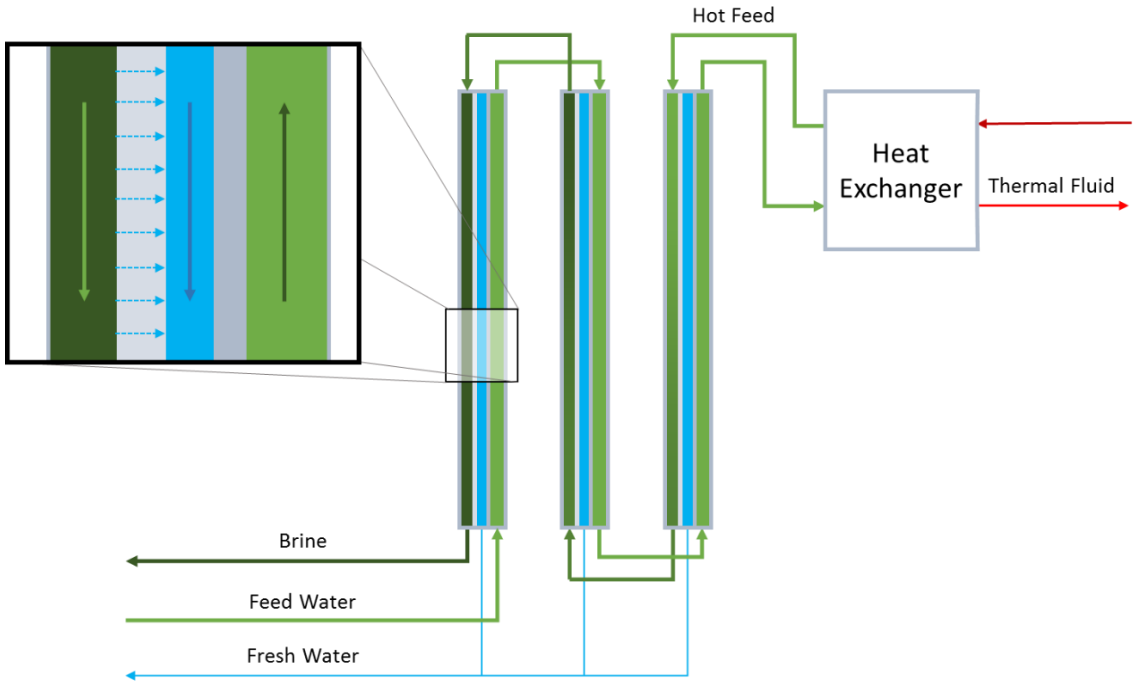

Figure 5: Multiple-effect membrane distillation diagram

1.2.2.4 Mechanical Vapor-Compression

MVC systems use electricity to drive a mechanical vapor compression pump that lowers the pressure in the feed chamber and compresses the vapors coming from the feed water. This produces heated fresh water, which is often used to heat the feed water bath. Heating elements are sometimes added to the feed water bath to increase yield.

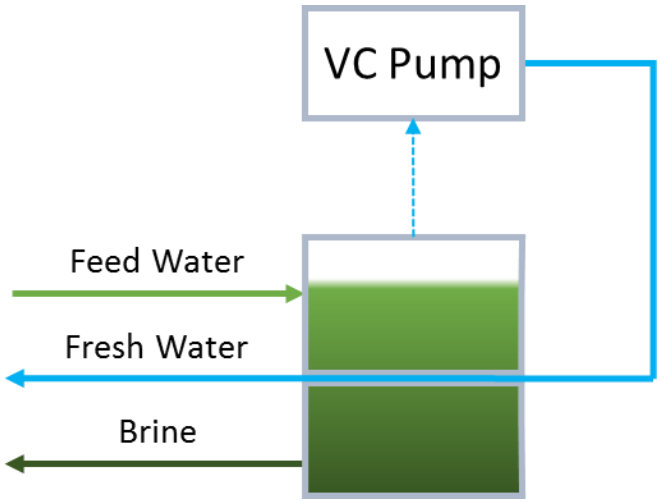

Figure 6: Mechanical vapor-compression diagram

1.3 Desalination Technology Comparisons

To get an idea of the differences in capabilities between the systems, the major categories are defined and compared. First we must find the common system properties, including redefining properties so proper comparisons can be made.

1.3.1 Efficiencies and Gain Output Ratios

To evaluate how effectively each system utilizes its input energy, we convert all the performance characteristics given into a standard efficiency. The efficiency of a system is defined as the amount of work done divided by the amount of energy used. The work done was already defined earlier and is the same for all of the systems.

Electrodialysis efficiencies are can be above 90% for systems that don't need to provide water of high purity (<100 ppm) [11] [12]. The high efficiency is achieved by the electrodes directly moving ions across membranes without any phase change or high pressures required. The downside is that with increased salt content the efficiency decreases because the brine begins to conduct electricity more and more effectively. This conductivity limits the salt concentration it can handle, although there are some systems that can handle higher salt concentrations. The explanation of the efficiency is outside the scope and field of this project and is not discussed further.

RO efficiencies for larger systems depend on the pressure needed to push percolate through the membrane. Some additional pressure beyond the osmotic pressure, called over-pressure, is needed to move any water through the membrane. Higher over-pressure means the system will run less efficiently, but produce water at a faster rate.

For seawater the incoming osmotic pressure is around 27 bar. To generate fresh water from seawater, a typical RO membrane typically uses 40 to 50 bar and recovers 25% to 50% of the feed water [13]. The resulting efficiency for a commercial reverse osmosis unit is between 50% and 70%.

Distillation systems are typically defined by their Gained Output Ratio (GOR). The GOR is defined as the amount of times steam is generated from the energy needed to evaporate water [14]. For example, an evaporator/boiler that does not condense the steam to heat up the incoming water or move air over the evaporating surface will never produce a GOR above 1. GOR values for the pressure-aided MSF systems can be above 20, with MED/MEMD systems being less effective.

To convert this to efficiencies, we can use the GOR and compare the energy required to evaporate water to the energy needed to overcome the osmotic pressure difference. The latent heat of water divided by the GOR is the energy required to evaporate water per kg. If we assume a GOR of 10 and convert the units to pressure, we get

$$\frac{2257kJ/kg}{10} = 226\frac{kJ}{kg} \quad (9)$$

The MSF systems also have an electrical requirement, being estimated around $10.0\frac{kJ}{kg}$. Given desalinating sea water theoretically takes only $2.7\frac{kJ}{kg}$, a 10 GOR system is only about 1.1% efficient. This sounds low, but these systems utilize a cheaper energy type and can handle higher salinity levels. At higher salinity levels, the efficiency can increase up to around 8% for large systems because it is doing more work while using about the same amount of energy for every kg of water produced [15].

1.3.2 Installation Costs

The installation costs are graded in relative terms, as it is difficult to find exact figures from many different manufacturers. As the systems covered are commercial technologies, the cost of producing the systems is often controlled by the materials used.

Electrodialysis, RO, and MVC systems are comparatively inexpensive and all run on electricity. The size of the systems are small, as not much surface areas are needed to transfer water. Only RO systems handle high pressures, meaning some more expensive piping and components are required in an installation.

MEMD is likely the middle. The membrane and structure can be made of inexpensive polypropylene. Also, the surface area for evaporation is large compared to the size of the unit due to the use of membranes in the place of air-gaps.

MSF and MED systems are fairly expensive, generally being made of large stainless steel structures. A significant amount of surface area is needed to facilitate water evaporation in both cases. MSF systems trade off needing less overall evaporation area with a higher energy requirement compared to MED

1.3.3 Salt Concentrations

Electrodialysis is limited by the voltage difference that can be maintained within the salty, conductive water. This leads to generally low salt concentrations, working most effectively at less than 6000 TDS [7] [12]. Additionally these systems are most effective at slight reducing the Total Dissolved Solids (TDS), and not handling water with high salt concentrations. The majority of commercial systems remove less than half of the salts from the percolate.

RO can generally handle higher salt concentrations. Pre-treatment of the water allows the system to handle higher concentrations than normal without the membrane clogging. The limit RO systems can handle with pre-treatment is around 60,000 TDS. RO systems generally leave around 0.5% of the salt in the percolate. This is only a concern if very pure water is desired as percolate.

Distillation systems are not generally affected by the salt concentrations and don't need pretreatment outside of low cost bio filters. Salt level can generally be tolerated until crystals begin to form in the brine. This happens between 120,000 and 180,000 TDS for most water sources. The percolate produced is usually very pure.

1.3.4 Additional Considerations

Aside from the electrical costs, RO membranes need to be periodically replaced and high pressure pumps maintained. Additionally, pretreatment for Electrodialysis and RO systems may also incur significant running costs (chemicals, particle filters, water softeners) [16] [6].

Pre-treatment methods are generally not suitable for dynamic conditions, such as farm runoff where the salt content in the water varies depending upon fertilizers, pesticides, etc. Distillation systems are more favorable in these situations, as the system is tolerant to a wider array of salts and is less susceptible to fouling.

1.3.5 Comparison Table

This is a table of approximate energy requirements. This does not include electrical needs for running pumps not related to the specific desalination process. An evaluation including these can be found in the references [17]. For the cost estimates, $0.10 per kWh electrical energy and $0.03 per kWh thermal energy.

Table 1: Desalination comparison table

System	Electro	RO	MVC	MSF	MED	MEMD
Electric Energy (kJ/kg)	0.1 – 0.3	0.5 – 7.5	15 – 25	7 – 14	-	-
GOR	-	-	-	6 – 12	6 – 10	5 – 8
Thermal Energy (kJ/kg)	-	-	-	190 – 380	230 – 380	260 – 450
Max Temperature (C)	-	-	-	120	90	70
Total Energy (kJ/kg)	0.1 – 0.3	0.5 – 7.5	15 – 25	197 – 394	230 – 380	260 – 450
Tolerated TDS (ppt)	0 – 6	3 – 60	60 – 120	60 – 120	60 – 120	60 – 120
Approx. Efficiency	50-95%	< 70%	< 60%	< 8%	< 6.5%	< 6.0%
Energy Costs ($/m3)	0.0067	0.11	0.55	2.65	2.82	2.96
Relative Install Cost	Low	Low	Low	High-Mid	High	Mid

1.4 Zero Liquid Discharge

Zero liquid discharge refers to no liquid brine exiting a desalination facility. This is generally achieved by adding another stage after the desalination steps. This stage takes the high salinity brine from a desalination system and produces salt solids. There are several ways to achieve this, but we will only cover the use of an evaporator and filter press combination.

1.4.1 Evaporator

The evaporator takes in high salinity water and evaporates water into the atmosphere [18]. Evaporators can be configured with multiple effects, having the steam from one effect warming up the brine in the next. The concentration increases until the salt is about to precipitate out of the brine. This salt concentrate, often only 10% of the original brine volume, can either be trucked away directly at a much lower cost or passed to another system on site to produce dry salt.

Evaporators are normally powered by either waste steam or natural gas. Some steam powered evaporators can be run by other heat sources by simply substituting the steam for thermal oil.

Substituting thermal oil for steam requires higher temperatures because the thermal energy is provided through a temperature change instead of a phase change. This conversion is covered in more detail in the evaporator demo section.

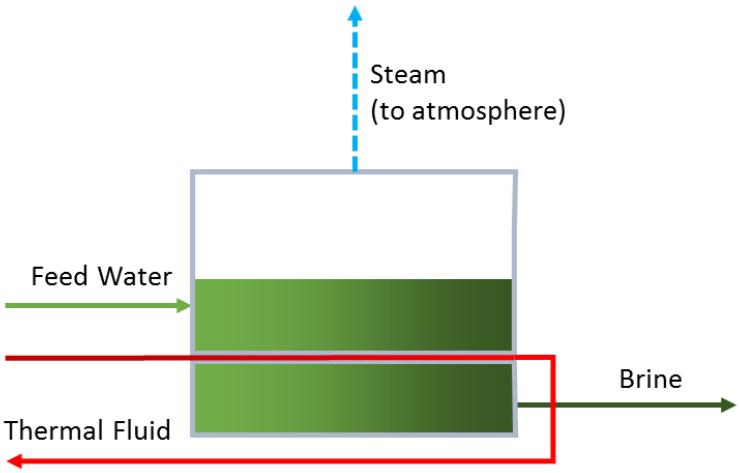

Figure 7: Evaporator diagram

1.4.2 Filter Press

There are a number of systems that can produce dry salts from salt concentrate. We will only focus on the filter press because it generally matches well with the salt concentrations leaving an evaporator. In a filter press, the brine is forced through a rubber membrane, leaving the precipitated salt crystals behind. After each batch, the filter press is opened up and the salt cakes drop into a collection bin.

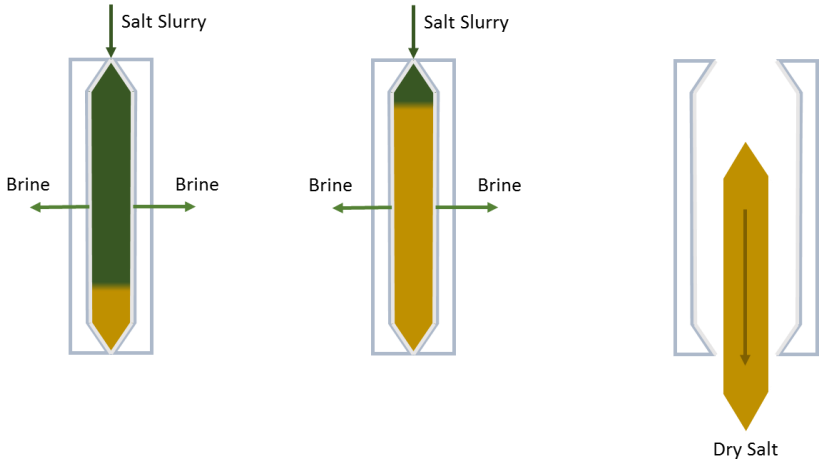

Figure 8: Single chamber of a filter press diagram

1.4.3 Zero Liquid Discharge Configuration

Below is a depiction of a thermal salt evaporator coupled to a bank of solar thermal collectors. This is one of the simplest ways to augment a system to have zero net discharge of salt water.

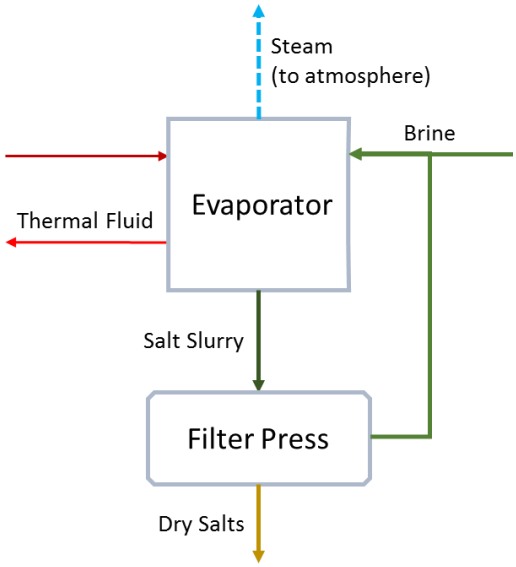

Figure 9: Evaporator and filter press combined diagram

1.5 Solar Thermal Collectors

Before delving into how solar thermal technology can be used with desalination technologies, solar thermal collector technologies will be covered. An exhaustive review of solar thermal energy systems has been described in previous articles [19] [20] [21] [22]. This thesis will cover the most prominent technologies as well as what technologies are being used and demonstrated at UC Solar.

A solar thermal collector is a device that captures thermal energy from sunlight. The collector generally consists of an absorber that converts solar rays into heat. Solar thermal collectors can include a concentrator that reflects light toward the absorber. The different collector types collect solar energy in different ways. All collectors absorb direct sunlight coming from the direction of the sun. Some collectors also absorb indirect sunlight reflecting off the atmosphere or clouds.

1.5.1 Non-Concentrating Collectors

Non-Concentrating solar thermal collectors are generally flat plate collectors. This type of collector is non-tracking and fixed in place. Generally these collectors consist of a solar absorbing surface facing the sun and covering a channel carrying thermal fluid, which will be collectively referred to as an absorber.

To reduce thermal losses, a glass layer is often placed above the coating to help retain heat and reflect thermal radiation back to the absorber. Insulation is also often installed on the back of the fluid channel to lower thermal losses from the surface not facing the sun. [23]

Collectors without concentration generally provide thermal temperatures below 100 ℃ [24]. The installations and operation of these systems are fairly simple, having few moving parts [23]. Solar thermal collector performance can vary greatly depending on the time of year and weather. Performance for non-tracking systems generally drop off more gracefully, being able to absorb direct and indirect sunlight.

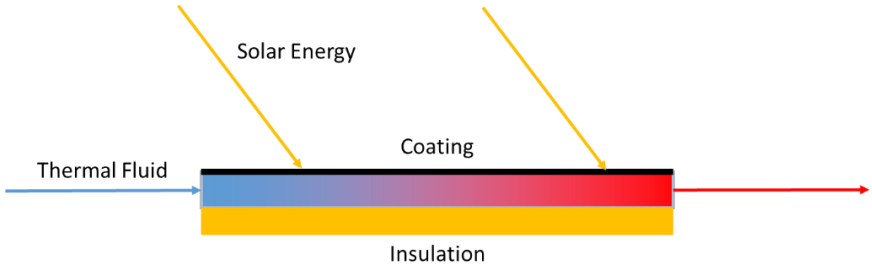

Figure 10: Basic flat plat solar collector diagram

1.5.2 Concentrating Collectors Without Tracking

Concentrating collectors also have an absorber. The difference is the addition of reflectors that direct additional sunlight toward the absorber, meaning more energy can be collected in a given area. These non-tracking variants of concentrating collectors are also fixed in place.

These systems can provide heat above 100 ℃. The installation of these systems aren't much more complex than that of flat plate collectors, aside from needing additional insulation and components that can operate at higher temperatures. Concentrator performance also drops off more gracefully in adverse weather, being able to absorb direct and some indirect sunlight [25].

In the UC Solar group, concentrators based off non-imaging optics designs are used for their high performance and non-tracking properties [26]. Specifically, several arrays of Compound Parabolic Concentrators (CPC) have been installed at UC Solar. The first image below is a 3D model of a CPC generated from a custom ray tracing program [27]. This shows how the reflector is able to reflect light towards the absorber. The black bar in the image is the absorbing surface, while the reflective outer surfaces is the concentrator. The second image on the next page shows part of a bank of CPCs deployed by the UC Solar group. This specific array consists of 160 collectors.

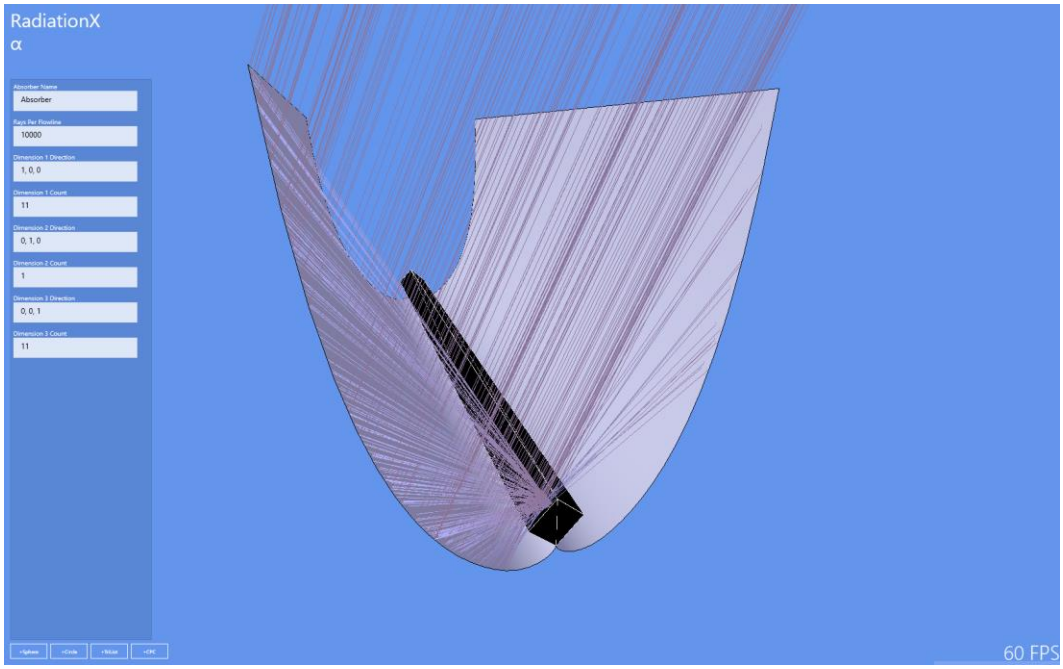

Figure 11: 3D rendering of a CPC with incoming rays

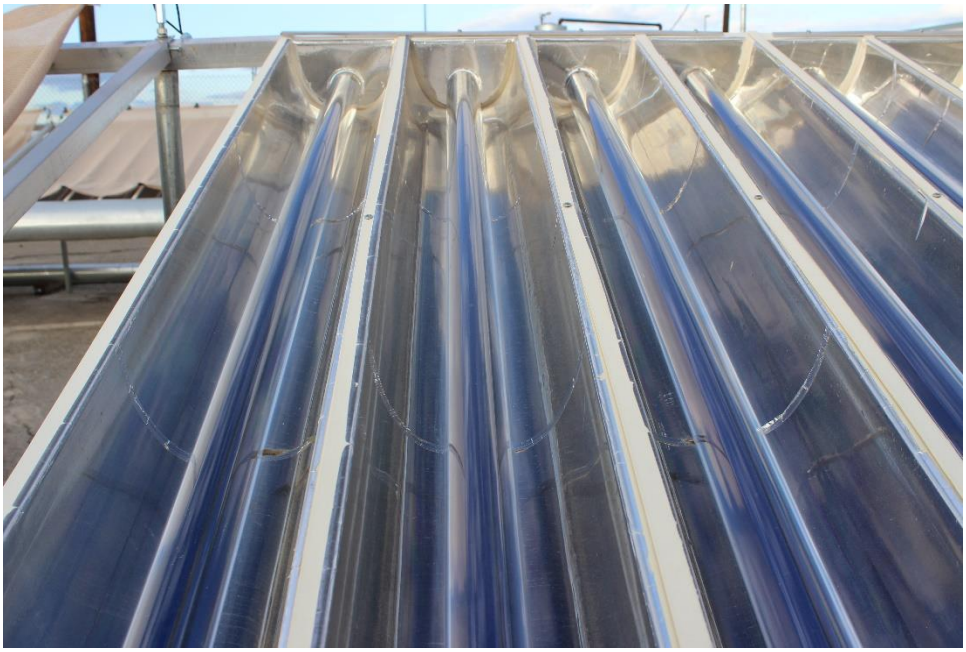

Figure 12: UC Solar CPC array close up

1.5.3 Concentrating Collectors With Tracking

Solar thermal concentrators with tracking have much the same design as those without tracking. The main difference is the concentrators and often the absorber move to track the sun through the sky. Moving, by tilting and panning, allows for additional solar thermal energy to be collected on the absorber surface.

Depending on the specific configuration and size, concentrating and tracking solar thermal collectors are able to achieve temperatures above $1000\ ℃$ [28]. The installation of such systems are considerably more complex with large moving concentrator surfaces and any necessary support structures. The performance of tracking solar thermal collectors are also very susceptible to small defects in the collector shape [29]. These collectors can suffer on cloudy days due to only being able to collect direct sunlight.

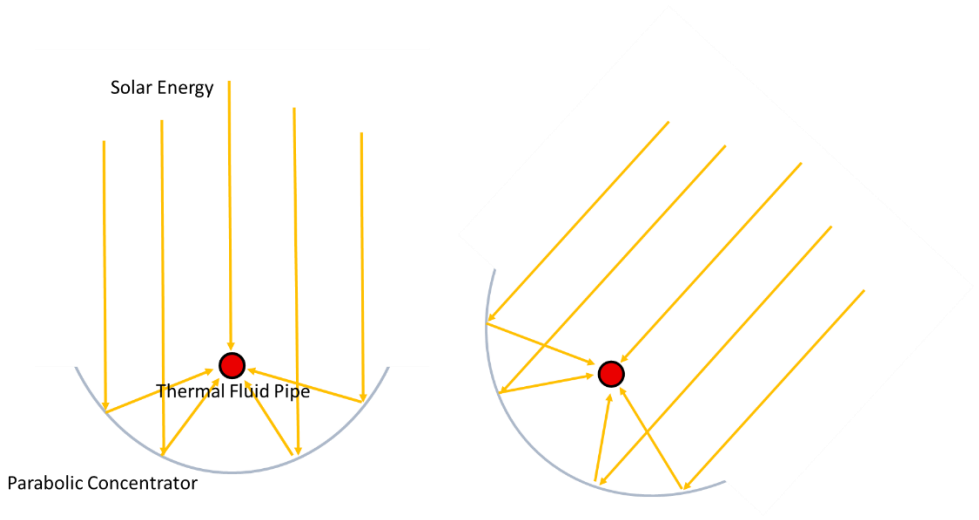

Figure 13: Parabolic solar tracking concentrator diagram

1.6 Existing Solar Thermal Installation

The existing solar thermal loop at UC Solar utilizes CPC collectors in an array, consisting of 160 individual collectors aligned in series and parallel. This array is capable of achieving thermal fluid temperatures up to 180 ℃ for 6 to 8 hours a day.

This is done by moving thermal oil, specifically Duratherm 600 [30], at 0.5 kg per second through the solar collectors. This increases the thermal energy in the oil by increasing its temperature. The thermal fluid is then sent to the device being powered, releasing thermal energy with a temperature drop. The thermal fluid then completes the loop back to the absorber, continuing to transfer thermal energy from the collectors to the thermally powered device.

These CPC collectors have demonstrated the ability to continue functioning even in cloudy conditions. Although the power provided can drop considerably, high temperatures can still be reached.

The thermal energy transfer is much more complex than described, involving convective, conductive, and radiative heat transfer. The specifics of how the energy flows through the system can be understood by studying the different transfer modes and the design of a specific solar thermal loop [31] [32].

Below is a simple solar array with 4 collectors in series. Each collector in the series increases the temperature of the thermal oil. Much like battery voltages in circuitry, collectors can be added to the series to attain a larger temperature difference. Collector banks can also be added in parallel to increase the total power of the array without increasing the temperature difference.

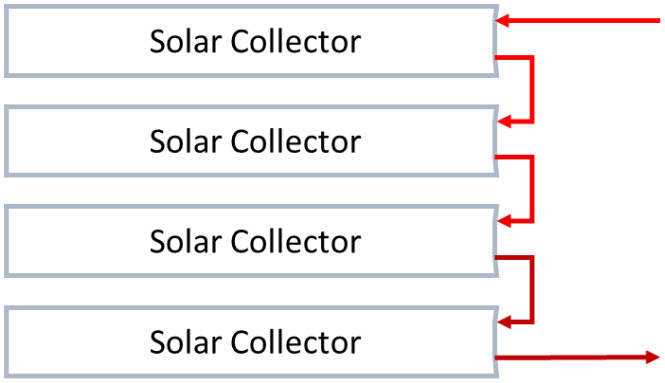

Figure 14: Solar thermal loop with 4 collectors.

2 Solar Thermal Evaporator Demo

As a scaled prototype of a desalination component working with solar thermal energy, the UC Solar group is considering installing an evaporator to its existing 25kW solar thermal loop. In practice, the evaporator ultimately may be a small part of an inland desalination installation. However, dealing with large volumes of concentrated brine is a critical capability when implementing large desalination systems.

Additionally, natural gas and steam powered evaporators are used for waste water concentration in many situations, reducing the overall volume of waste water for cost savings [18]. These systems are well understood and pose little risk. Driving an evaporator with solar thermal energy is a new approach and has some operational unknowns. This combination may prove to be a practical way to reduce the environmental impacts over traditional evaporator installations.

This demo has not been built yet, but a simulation has been developed to evaluate expected performance. This evaluation is to be included in a proposal for the California Department of Water Resources.

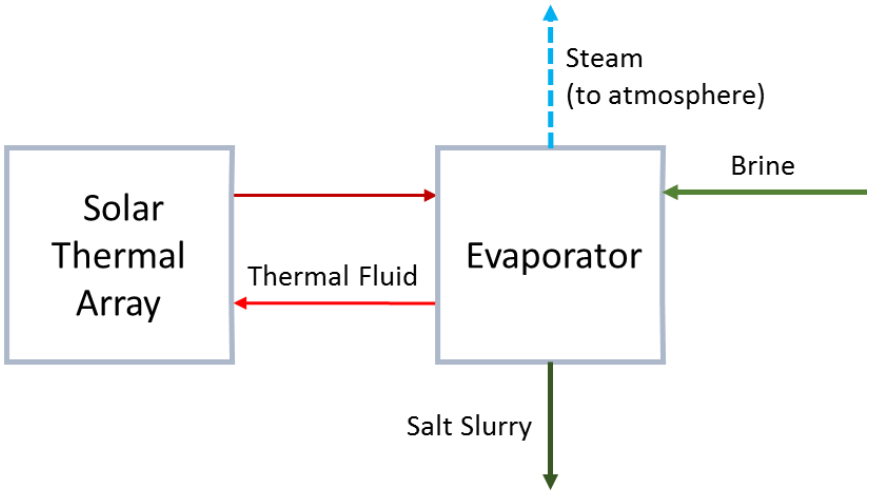

Figure 15: Solar thermal array and evaporator loop

2.1 Evaporator Integration

When integrating an evaporator into a solar thermal loop, there are two main approaches that were considered. One approach is to attempt to drive an evaporator as if it was running off a constant heat source. This will require additional solar thermal power to provide the energy needed to run the system when solar thermal energy isn't collected over night. This first approach also requires a way of storing solar thermal energy, usually with tanks, and additional piping and controls to provide a constant source of energy to the system being run by the solar thermal energy. The evaporator should ultimately perform as it was powered by a constant energy source.

A second approach is to directly link the solar thermal energy loop to the evaporator. This requires no thermal storage tanks, but can have a significant impact on the evaporator performance. The fact that this second approach would be a simpler, and less expensive to install, made it the first choice. Going this route also allows us to assess the effects of powering an evaporator with a dynamic thermal energy source.

Without the need for large thermal storage equipment, the evaporator can be integrated into the current solar loop close to the current piping. This piping has existing valves that allow the control and shut off of other components in the loop. Adding the evaporator would require using taps that have already been made, or by tapping the loop in a more useful location. The image below shows the current configuration of the solar thermal loop where the evaporator would hook into. There is a good location on the far side of the pump that is close to the loop and is easily accessible.

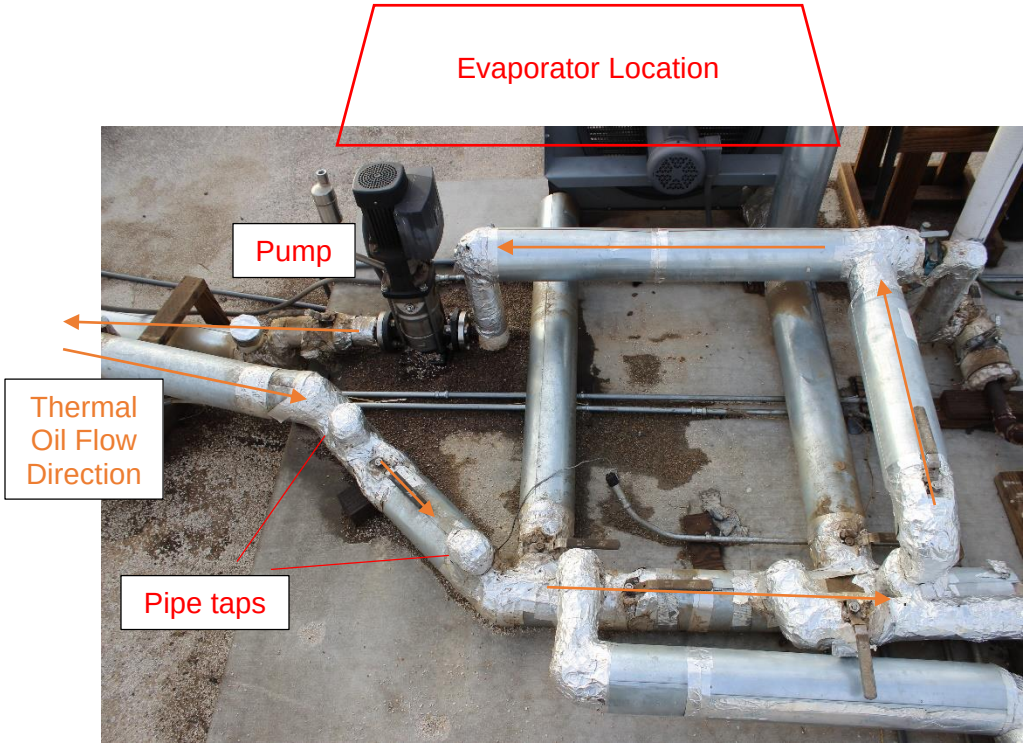

Figure 16: Solar thermal loop end with pump

An evaporator needs to be selected that can perform well with 20 kW of thermal energy. Evaporators are usually sized based upon the amount of water that is evaporated over time. The calculation used to estimate the volume of water evaporated is mostly defined by the latent and specific heat of water. Estimating an input temperature of 25 C and a boil temperature of 100 C, we can evaluate:

$$P\left(\frac{1}{C_P + s_p \Delta T}\right) = \dot{m} \qquad (10)$$

$$20\ \text{kW} * \frac{3600\ \text{sec}}{\text{hour}} * \left(\frac{1\ \text{kg}}{2257\ \text{kJ} + 4.2\frac{\text{kJ}}{K} * 75\ K}\right) = 28\frac{\text{kg}}{\text{hour}} \qquad (11)$$

This gives an estimate to help find an appropriate evaporator size. An evaporator from ENCON Evaporators [18] will be focused on, having a rated capacity of 38 kg per hour. This specific evaporator was designed to run on $150\ ℃$ steam, but can accept thermal oil as well. A system having up to double the capacity ($\sim 55\ \text{kg/hour}$) might not be wasted as the current solar loop will be expanded in the future.

To ensure that the system will perform correctly, the temperature needs must also be considered. To find these temperatures, we need to know more about this specific evaporator.

2.1.1 Evaporator configuration

The evaporator selected has an insulated brine chamber that can hold about 0.7 cubic meters of brine. The heat exchanger consists of 4 plates measuring approximately 0.50 x 0.35 meters, giving an effective surface area of 1.4 square meters. The heat exchanger is fully submerged in the evaporator's brine bath. The inlet and outlet pipes for the heat exchanger are 5 cm in diameter. The evaporator also has an air pump to move the steam out of the evaporator and a demister to ensure entrained liquid droplets do not escape to the atmosphere.

Figure 17: ENCON 38 kg per hour evaporator

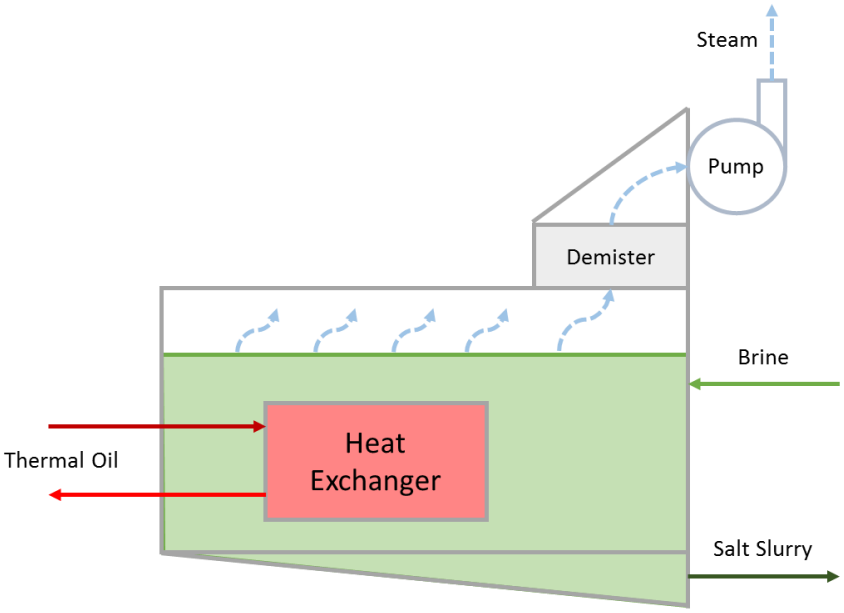

Figure 18: Evaporator configuration

2.1.2 Steam Configuration Check

To estimate the needed temperature of the ENCON evaporator [18], heat transfer rates are calculated with steam and mineral oil in the heat exchanger. These calculations ensure that the temperature requirement for thermal oil can be met. This also provides a check to ensure the evaporator can perform as the specification sheet indicates. The specification sheet states that the heat exchanger within the evaporator has 4 plates measuring approximately 0.50 x 0.35 meters, giving a total surface area of 1.4 square meters. The specification sheet also shows an evaporation rate of 38 kg per hour.

The first check is to estimate the heat exchanger heat transfer coefficient and ensure it is a reasonable value. A few assumptions are made to perform this: a uniform wall temperature of $150\ ℃$ for the heat exchanger walls, an inlet brine temperature of $25\ ℃$ into the bath, a temperature of $100\ ℃$ for the brine, and a brine evaporation rate of 38 kg per hour. The total power transferred from the heat exchanger can be found by rearranging equation 10 and solving for power:

$$38\frac{\text{kg}}{\text{hour}} * \frac{1\ \text{hour}}{3600\ s} * \frac{2257\ \text{kJ} + 4.2\frac{\text{kJ}}{K} * 75\ K}{1\ \text{kg}} = 27\ \text{kW} \qquad (12)$$

The heat transfer coefficient can now be found by taking into account the temperature difference and the estimated area of the heat exchanger. We start with this heat exchanger equation and solve for the heat transfer coefficient [33]:

$$h = \frac{q}{A(T - T_\infty)} \qquad (13)$$

$$\frac{27\ \text{kW}}{1.42\ m^2 * (150 - 100)K} = 380\frac{W}{m^2\ K} \qquad (14)$$

This heat transfer coefficient of this value is well within the expected value of a heat exchanger immersed in boiling water [34]. Finding this value completes the check and indicates the evaporator should perform as advertised.

2.1.3 Mineral Oil Configuration Check

To estimate the energy transfer through a heat exchanger using thermal mineral oil [30], the same assumptions cannot be made. Due to the fluid not undergoing a phase change, we can't assume a constant heat exchanger wall temperature. It is still possible to provide the 28 kW of thermal power, but a higher oil temperature will be required.

To evaluate the input and output temperature of the mineral oil, equation 13 still applies. The difference is the temperature of the mineral oil drops as it moves through the heat exchanger. The new equation that handles the drop in temperature is along the heat exchanger is:

$$\frac{\Delta T}{A} = \frac{q}{s_p \dot{m}} \qquad (15)$$

Evaluating the equations was done by integration or by breaking down heat exchanger into small sections as done in the appendix. The calculations show the temperature of the inlet oil will be about 168 ℃ and an outlet temperature of 136 ℃. This shows that an appropriately sized, non-tracking solar loop will be able to provide the thermal energy to run the evaporator as effectively as steam.

We can also use the heat exchanger temperatures to find the effectiveness. The effectiveness of a heat exchanger is the amount of thermal energy provided compared with the theoretical thermal energy it can provide. The oil inlet temperature is 169 ℃ and the brine bath undergoing a phase change is 100 ℃. The total energy that can be transferred into the brine is:

$$Q_{\max} = s_p \cdot m \cdot \Delta T = 1.67 \left(\frac{kJ}{kg\ K}\right) \cdot 0.5 \left(\frac{kg}{s}\right) \cdot 69(K) = 58\ kW \qquad (16)$$

Compared to the actual heat transfer rate of 27 kW for the heat exchanger, the effectiveness of the heat exchanger can be found [33]:

$$\varepsilon = \frac{Q}{Q_{\max}} = \frac{27\ kW}{58\ kW} = 0.47 \qquad (17)$$

2.2 Estimated Performance

Combined with the current solar loop power of 20 kW, we expect to have lower performance than if 27 kW of thermal power was provided. The assumption is that the drop off in performance is approximately linear when providing reduced thermal power. This is just a value to check against the simulation, not a final value. This gives a simple evaporation rate estimate:

$$38\ \frac{\text{kg}}{\text{hr}} * \frac{20\ \text{kW}}{27\ \text{kW}} = 28\ \frac{\text{kg}}{\text{hr}} \qquad (18)$$

To now find the approximate input temperature, equations 16 from the mineral oil configuration check can be used. Doing so shows that the system should run at an input oil temperature of $154\ ℃$. This lower temperature is expected, given our heat exchanger is dissipating less energy. Additionally, an increase in performance may be seen from the solar loop since it performs more efficiently at lower temperatures.

The effectiveness of our heat exchanger at boiling can be estimated to be 0.44, shown by evaluating the equation 16 and 17 from above.

$$Q_{\max} = s_p \cdot m \cdot \Delta T = 1.67\ \left(\frac{kJ}{kg\ K}\right) \cdot 0.5 \left(\frac{kg}{s}\right) \cdot 54(K) = 45\ kW \qquad (19)$$

$$\varepsilon = \frac{Q}{Q_{\max}} = \frac{20\ kW}{45\ kW} = 0.44 \qquad (20)$$

With a capacity of 0.7 cubic meters, it would take about 4 hour to heat up brine to $100\ ℃$, as shown in the following equation:

$$t = \frac{s_p \cdot V \cdot \rho \cdot \Delta T}{Q} = \frac{4.2 \frac{kJ}{kg\ K} \cdot 0.7\ m^3 \cdot 1000 \frac{kg}{m^3} \cdot 75\ K}{20 \frac{kJ}{s}} = 3.1\ hours \qquad (21)$$

This does not mean that the evaporator will only be effective for the last few hours of the day, but it will evaporate at a slower rate before and after boiling occurs.

The achievable concentration of the salt slurry leaving the evaporator is dependent on the salts in the incoming brine. That concentration is usually between a TDS of 220,000 ppm and 320,000 ppm, depending on the salt mixture. The final TDS for an installation is usually determined by performing a boil test in a laboratory environment.

In this example we estimate the salt mixture will be farm runoff, estimated by salt the spikes in the local river [3].

Ion/Anion	Molar Percentage
Sodium	44%
Chloride	33%
Calcium	10%
Sulfate	7%
Other	6%

Sodium (Na^{+}) chloride (Cl^{-}) salt makes up the majority of the salts in the water. Additionally the calcium (Ca^{2+}) when the salt spikes is near precipitation levels ($52 \text{ vs } 70 \text{ mg/L}$), only needing to combine with carbonate ions (CO_3^{2-}) in the brine to precipitate out of the solution into calcium carbonate scale (limestone). In other words, the calcium will precipitate out of the brine with only slight increases to salt concentration.

The evaporator is designed to function until suspended salts solids in the brine are present in some quantity. It is also able to function after small levels of salts, such as calcium carbonate, have begun to scale on the surfaces inside the evaporator. If the concentration is too high and other salts begin to precipitate out, excessive scaling can occur and rapidly reduce the effectiveness of the evaporator.

2.3 Simulation

To estimate the performance of an evaporator being powered by a solar thermal loop, a simulation was developed. This allowed the testing of ideal scenarios and coupled with data from a working solar thermal loop. The calculation in the previous section are used for additional error checking of the simulation.

2.3.1 Energy Balance

To handle the energy balance each major energy sources and sinks. Two energy balances are simulated concerning the solar thermal loop oil temperature and the evaporator brine temperature. These are modified to be based on heat transfer rather than energy in this simulation. The oil loop equation and the brine heat transfer equations are respectively:

$$\Delta Q_{\text{oil}} = Q_{\text{col}} - Q_{\text{env}} - Q_{\text{brine}} \quad (22)$$

$$\Delta Q_{\text{brine}} = Q_{\text{brine}} - Q_{\text{env}} - Q_{\text{evap}} \quad (23)$$

For the solar thermal loop oil equation, the solar energy collected is the main input and is defined by data or as a constant energy source. Increasing the heat energy in the solar thermal loop increases the oil temperature. This gives the oil temperature difference between the inlet and outlet of the collectors.

$$\Delta T_{\text{oil}} = \frac{Q_{\text{col}}}{s_{p\ \text{oil}}\ \dot{m}_{\text{oil}}} \quad (24)$$

Energy lost in the loop is the energy lost through the piping of the solar thermal oil loop. This is simplified by creating working constant to simplify the calculation on simulation run time. With an estimate of the oil temperature and ambient temperature, the heat transfer lost can be estimated and lowers the temperature of the oil in the loop.

$$\frac{k_{\text{pipe}}\ A_{\text{pipe}}\ (T_{\text{oil}} - T_{\text{env}})}{d_{\text{pipe}}} = Q_{env} \quad (25)$$

The energy transferred to the brine is the thermal energy that transfers from the oil through the heat exchanger walls in the evaporator. This is driven by the temperature difference between the oil and the brine.

$$h = \frac{k}{d} = C, \qquad h_{\mathrm{HX}\,0}\, A_{\mathrm{HX}}\, (T_{\mathrm{oil}} - T_{\mathrm{brine}}) = Q_{\mathrm{brine}} \tag{26}$$

To account for scale formation on the heat exchanger, the heat exchanger conductivity can be altered to include the effect of the scale. Using the theory of thermal resistances being additive, we find the thermal resistances of the heat exchanger without scale and the resistance of the scale itself.

$$C = \frac{1}{R} \qquad R_{\mathrm{HX}} = R_{\mathrm{HX}\,0} + R_{\mathrm{scale}} \tag{27}$$

$$R_{\mathrm{HX}\,0} = \frac{\Delta T}{q} = \frac{A_{\mathrm{HX}}\, \Delta T}{Q_{\mathrm{brine}}} = \frac{1}{h_{\mathrm{HX}\,0}} \tag{28}$$

$$R_{\mathrm{scale}} = \frac{d_{\mathrm{scale}}}{k_{\mathrm{scale}}} = \frac{1}{h_{\mathrm{scale}}} \tag{29}$$

Solving equation 23 starts with the heat transferred to the brine in equation 26. Much like equation 25, the heat loss through the walls is calculated based upon the temperature of the brine inside the evaporator and the ambient temperature.

$$\frac{k_{\mathrm{ins}}\, A_{\mathrm{ins}}\, (T_{\mathrm{brine}} - T_{\mathrm{env}})}{d_{\mathrm{ins}}} = Q_{\mathrm{env}} \tag{30}$$

The brine evaporation heat transfer is calculated based upon common evaporation rate data. This data correlates the evaporation rate per area with the surface temperature of the brine [35]. In the presence of high salt concentrations, the boiling temperature increases slightly, which is taken into account in the simulation.

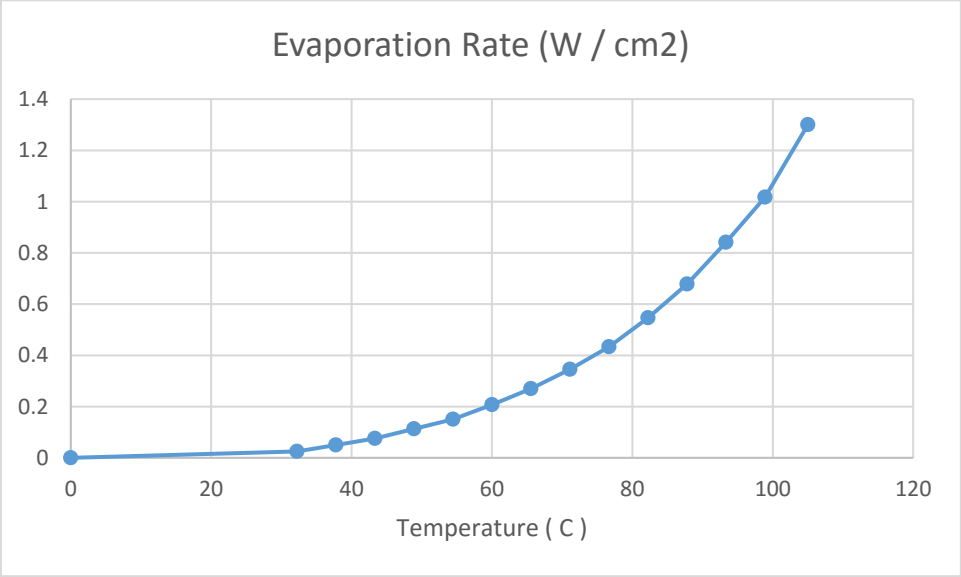

Figure 19: Evaporation rate vs. surface temperature

Once the brine is above boiling, the heat transfer equation changes from being based upon the surface area of the brine to being based upon the surface area of the heat exchanger. The jump in heat transfer is substantial enough that the brine effectively does not increase above its boiling temperature.

With equation 22 and 23 solved, the power gained by each is used to increase the starting temperature of the next simulation cycle. To compensate for new brine entering the evaporator, the final temperature is reduced using equation 33. This completes the energy balance equations.

$$T_{\text{oil}\,n+1} = T_{\text{oil}\,n} + \frac{\Delta Q_{\text{oil}}\,\Delta t}{s_{p\ \text{oil}}\,m_{\text{oil}}} \qquad (31)$$

$$T_{\text{brine}} = T_{\text{brine}\,n} + \frac{\Delta Q_{\text{brine}}\,\Delta t}{s_{p\ \text{brine}}\,m_{\text{brine}}} \qquad (32)$$

$$T_{\text{brine}\,n+1} = \frac{T_{\text{brine}}\,m_{\text{brine}} + T_{\text{brine inc}}\,m_{\text{brine inc}}}{m_{\text{brine}} + m_{\text{brine amb}}} \qquad (33)$$

2.3.2 Mass Balance of Brine

The water evaporated is resupplied continuously by the same brine that was initially in the evaporator, keeping the brine mass inside the evaporator constant.

$$0 = m_{\text{brine inc}} - m_{\text{water evap}} \quad (34)$$

2.3.3 Mass Balance of Salt

The salt continues to accumulate in the evaporator, which increases slowly over the course of weeks.

$$m_{\text{salt}} = m_{\text{salt } n} + m_{\text{salt inc}} \quad (35)$$

This simple salt mass equation is complicated by the fact that a low solubility salt is present, being Calcium Carbonate (CaCO3). To deal with this, it is assumed that any new calcium that is added will turn into calcium carbonate scale and be deposited evenly on all surfaces in contact with the brine.

$$m_{\text{salt } n+1} = m_{\text{salt } n} + m_{\text{salt inc}} - m_{\text{calc inc}} \quad (36)$$

$$d_{CaCO_3} = \frac{m_{CaCO_3}}{\rho_{CaCO_3} A_{\text{wall brine}}} \quad (37)$$

2.3.4 Results

The simulation inputs consist of 2 example (ideal) data sets and 4 data sets based upon actual performance data of the UC Solar thermal loop. This gives a range of information that helps validate the simulation and some expected performance metrics from this evaporator connected to the current solar thermal loop at UC Solar.

The first simulation with test data is to find the overall performance of the system at its factory rated output of $38\ kg/hr$ of water mass evaporation [18]. According to the simulation it takes around 3 hours to warm up the evaporator.

It appears that 29 kW thermal energy is needed to provide the 27 kW to the evaporator. Some of this 27 kW is used to heat up and boil the brine, while some is lost through the evaporator walls.

It is interesting to note the performance changes when the brine begins to boil in the evaporator. While boiling, as much as 24 kW is being used to boil the water, giving a short-term efficiency of 89%.

$$\varepsilon = \frac{Q_{\mathrm{HX}}}{Q_{\mathrm{evap}}}, \qquad 89\% = \frac{24\ \mathrm{kW}}{27\ \mathrm{kW}} \tag{38}$$

Additionally the evaporation rate more than doubles from a maximum of $16\ kg/hr$ to a steady $38\ kg/hr$ when boiling occurs.

It is also important to note that the brine continues to evaporate well after the system has cooled down, at a significantly reduced rate. The overall evaporator efficiency for the 16 hours is around 67%. The reduced efficiency is mostly due to the evaporator continuing to lose energy to the environment while the brine evaporates at a much slower rate when not boiling.

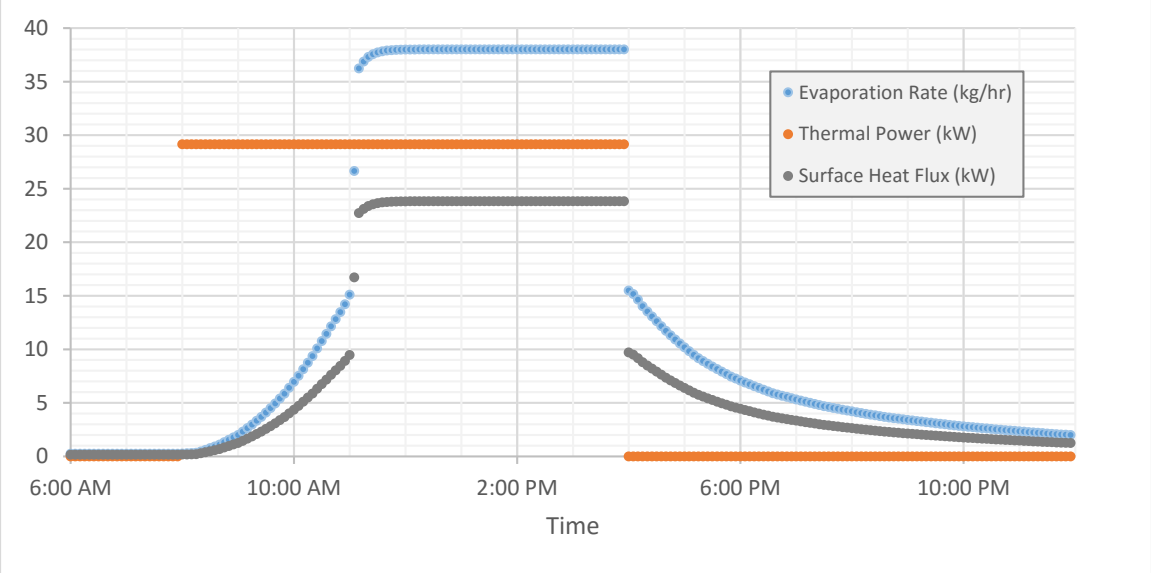

Figure 20: Simulation performance with constant thermal power over 8 hours

For the second simulation with example data, a more realistic sinusoidal curve was placed on the thermal input to better represent a solar thermal power profile. In this case it takes over 4 ½ hours to begin boiling. Additionally, boiling is only achieved for 2 hours.

The overall efficiency seen in this simulation is 57% over a 16 hour period. This additional drop in performance is mostly due to the short amount of time that the brine is boiling as comparison to the first simulation (Figure 20).

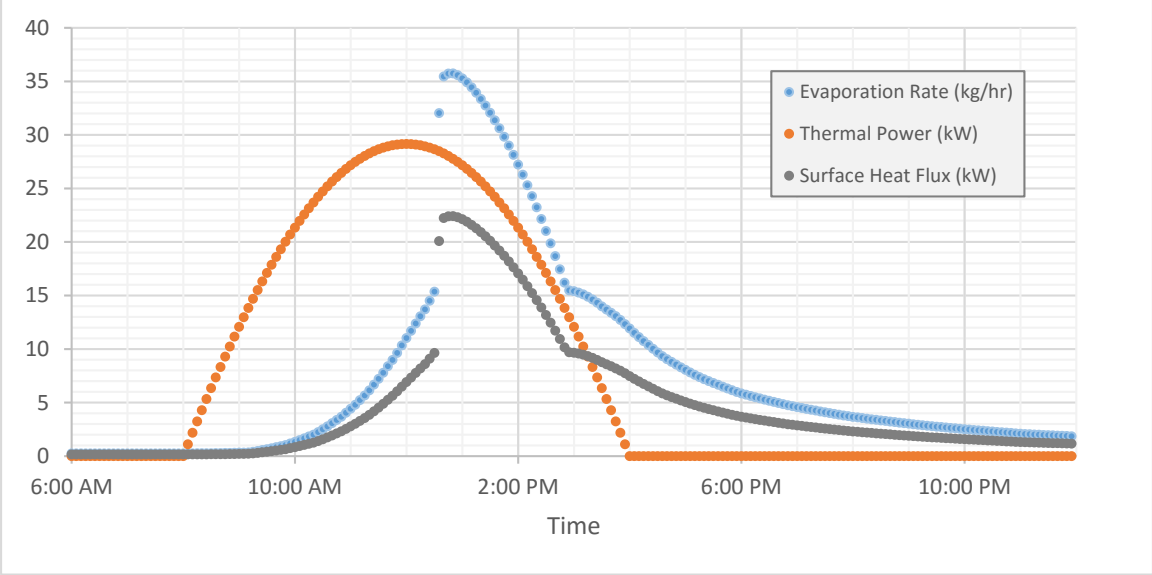

Figure 21: Simulation performance with sinusoidal thermal power curve over 8 hours

The remaining 4 simulations use data gathered from the UC Solar non-tracking thermal collector array. This collector array is undersized for this evaporator, but does provide an effective amount of energy to run the evaporator. None of these simulations indicated that the evaporator would have started boiling the brine.

There are a couple other interesting things to note in these simulations. The warm up time for the thermal loops would not be so apparent when connected to an evaporator. This dip in the thermal power at the beginning of the day is caused by no load being applied to the thermal loop, while an evaporator would be able to make use of low thermal power and would apply a thermal load during warm up.

Another interesting thing to note is the ability of the system to continue to perform on a cloudy day (Figure 24). This is mostly due to the non-tracking solar collector being able to collect indirect solar thermal energy in adverse weather.

The efficiency of the evaporators in these simulations are between 51% and 47%.

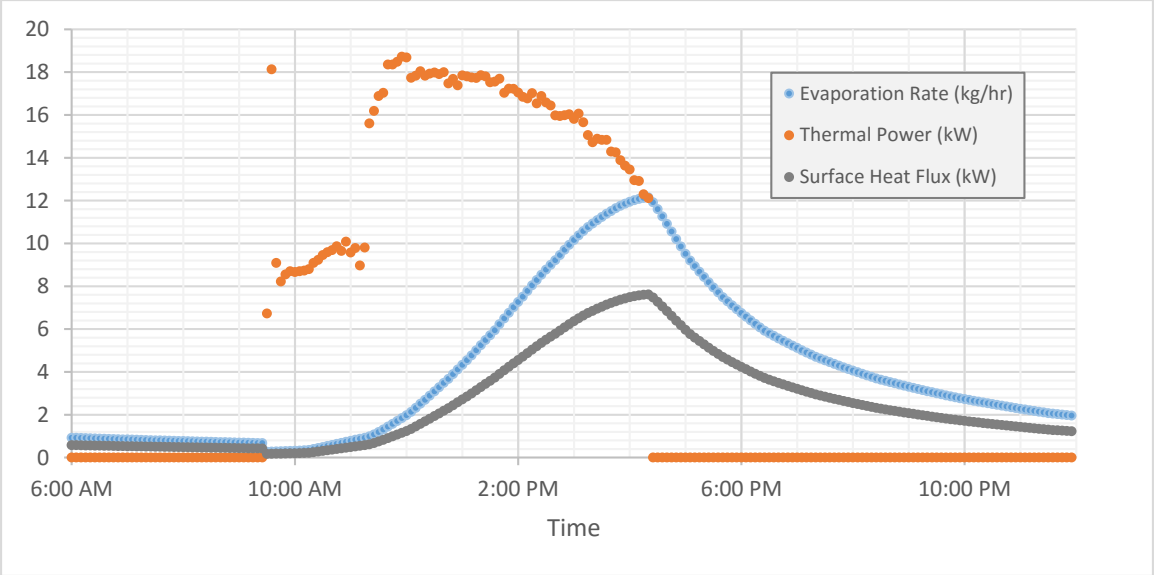

Figure 22: Simulation performance with solar thermal data (1/4)

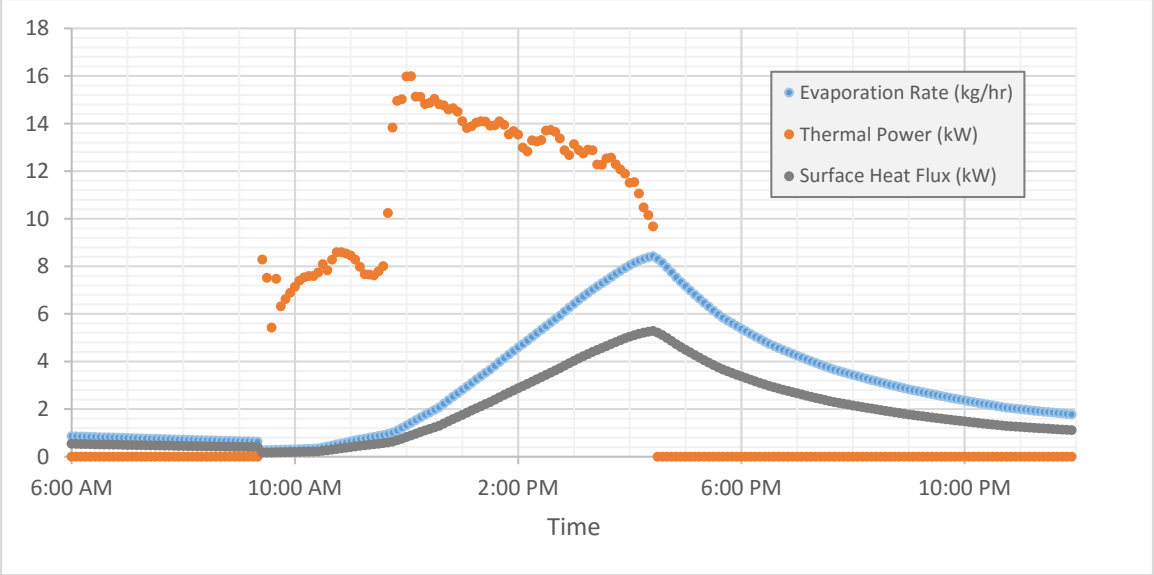

Figure 23: Simulation performance with solar thermal data (2/4)

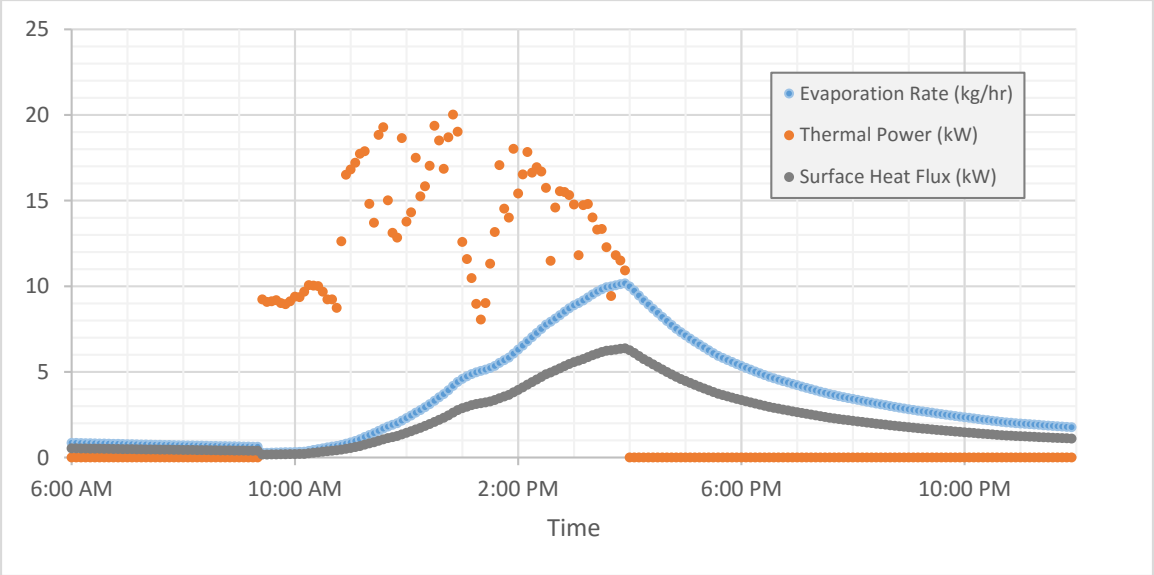

Figure 24: Simulation performance with solar thermal data (3/4)

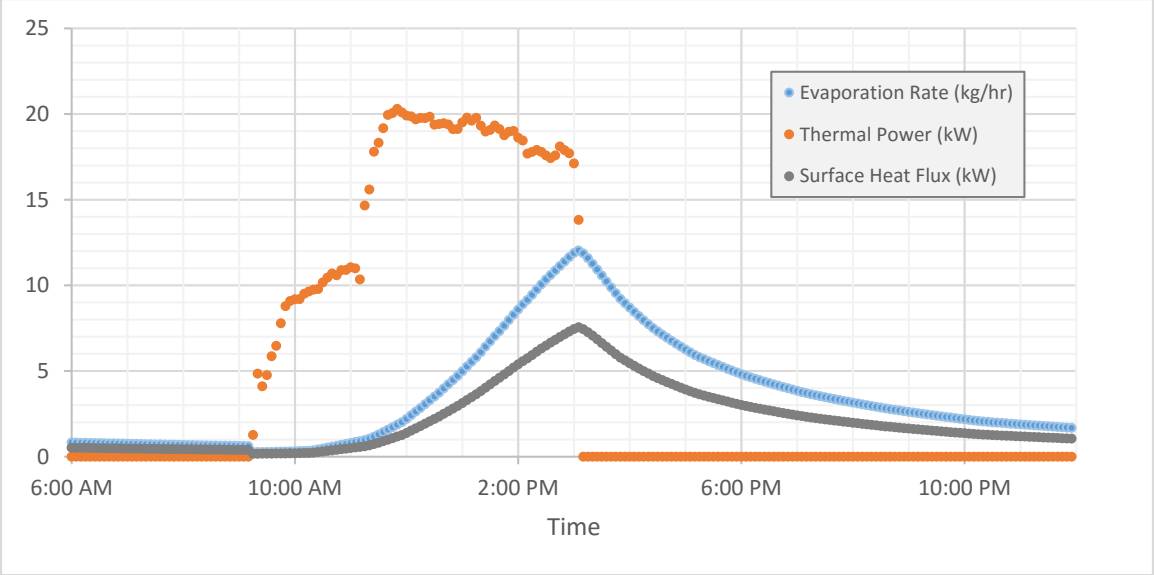

Figure 25: Simulation performance with solar thermal data (4/4)

3 Conclusion

According to the sinusoidal ideal data simulation (Figure 21) and utilizing equations 26 through 28, it would take about 370 days to reduce the heat transfer coefficient of the heat exchanger by 10%. Therefore as long as the evaporator is run correctly and this is an acceptable loss in performance, it should only need cleaning once a year or less.

The simulations show how important it is to correctly size the collector array to the evaporator component. It is still possible to test an oversized evaporator with an existing solar array, but a noticeable decrease in performance should be expected if the brine is never able to reach boiling temperatures.

From this information, future studies including evaporator systems integrated into the UC Solar infrastructure should include analysis of thermal storage. A way of keeping the evaporator running when the solar thermal energy is not collected could increase the efficiency and total evaporation mass significantly.

Overall solar thermal collectors can be used with evaporation technologies. Configuring an evaporator directly with a solar thermal loop is possible, but efficiency losses should be expected. This efficiency drop can be attributed to the limited hours of thermal energy available in such a configuration, not to any inherent limitation of solar thermal technologies.

4 Nomenclature

Following the definition of each variable, generalized units are given in terms of length (*L*), mass (*M*), time (*t*), and temperature (*T*).

$A =$ area, L^2

$C =$ thermal conductivity, M/t^3T

$C_p =$ latent heat capacity at constant pressure, ML^2/t^2

$d =$ thickness, L

$h =$ heat transfer coefficient, M/t^3T

$k =$ thermal conductivity, ML/t^3T

$M =$ molarity, mol/M

$m =$ mass, M

$\dot{m} =$ mass flow rate, M/t

$P =$ Power, ML^2/t^3

$Q =$ rate of heat flow across an area, ML^2/t^3

$q =$ heat flux, M/t^3

$R =$ gas constant, ML^2/t^2T mole

$R =$ thermal resistance, t^3T/M

$s_p =$ specific heat capacity at constant pressure, ML^2/t^2T

$T =$ temperature, T

$t =$ time, t

$\rho =$ density, M/L^3

$\Pi =$ osmotic pressure, M/Lt^2

References

[1] Carlsbad Desalination Project, Nov 2014. [Online]. Available: http://carlsbaddesal.com/.

[2] Department of Water Resources, "California Water Plan Update 2013," State of California, 2014.

[3] Department of Water Resources, July 2014. [Online]. Available: http://www.water.ca.gov/.

[4] R. Dashtpour and S. N. Al-Zubaidy, "Energy Efficient Reverse Osmosis desalination Process," *International Journal of Environmental Science and Development,* 2012.

[5] DOW, "FILMTEC Membranes Addendum: Osmotic Pressure of Sodium Chloride," 2014. [Online]. Available: http://www.dow.com/webapps/lit/litorder.asp?filepath=liquidseps/pdfs/noreg/609-02132.pdf&pdf=true.

[6] Lenntech, "Osmotic Pressure Calculator," 10 June 2014. [Online]. Available: http://www.lenntech.com/calculators/osmotic/osmotic-pressure.htm.

[7] R. P. Allison, "High Water Recovery with Electrodialysis Reversal," in *1993 AWWA Membrane Conference*, Baltimore, 2010.

[8] M. A. A.-G. Ibrahim S. Al-Mutaz, "Performance of Reverse Osmosis Units at High Temperature," King Saud University, Riyadh, 2001.

[9] SIDEM Veolia, "Multiple Stage Flash Process," June 2014. [Online]. Available: http://www.sidem-desalination.com/en/Process/MSF/.

[10] "memDist 6-52," July 2014. [Online]. Available: http://www.memsys.eu/dateien/products/memsys_datasheet_6_52.pdf.

[11] EET Corporation, "HEED Current Utilization Efficiency," 02 May 2015. [Online]. Available: http://www.eetcorp.com/lts/graph_HEED1.htm.

[12] GE Power & Water, "Electrodialysis Reversal (EDR)," 02 May 2015. [Online]. Available: file:///C:/Users/mafia/Downloads/FS1242EN.pdf.

[13] U. Lachish, "Optimizing the Efficiency of Reverse Osmosis Seawater," May 2002. [Online]. Available: http://urila.tripod.com/Seawater.htm.

[14] Kansas State University, "Gained Output Ratio," 02 May 2015. [Online]. Available: http://faculty.ksu.edu.sa/Almutaz/Documents/Gained%20Output%20Ratio.pdf.

[15] O. A. Hamed, "THERMAL PERFORMANCE OF MULTISTAGE FLASH DISTILLATION PLANTS IN SAUDI ARABIA," in *The Value of Water in the 21st Century*, San Diego, 1999.

[16] R. Y. Ning, "Discussion of silica speciation,fouling, control and maximum reduction," *Desalination,* pp. 67-73, 2003.

[17] "Energy Requirements of Desalination Processes," 19 Aug 2013. [Online]. Available: http://www.desware.net/desa4.aspx.

[18] Encon, "Thermal Evaporators," June 2013. [Online]. Available: http://www.evaporator.com/thermal-evaporator.

[19] Y. Tian and C. Y. Zhao, "A review of solar collectors and thermal energy storage in solar thermal applications," *Applied Energy,* pp. 538-553, 2013.

[20] P. G. Charalambous, G. G. Maidment, S. A. Kalogirou and K. Yiakoumetti, "Photovoltaic thermal (PV/T) collectors: A review," *Applied Thermal Engineering,* pp. 275-286, 2007.

[21] T. T. Chow, "A review on photovoltaic/thermal hybrid solar technology," *Applied Energy,* pp. 365-379, 2010.

[22] H. A. Zondag, "Flat-plate PV-Thermal collectors and systems: A review," *Renewable and Sustainable Energy Reviews,* pp. 891-959, 2008.

[23] J. Dara, K. Ikebudu, N. Ubani, C. Chinwuko and O. Ubachukwu, "Evaluation of a Passive Flat-Plate Solar Collector," *International Journal of Advancements in Research & Technology, Volume 2, Issue 1, January,* 2013.

[24] A. H. Abdullah and A. A. Ghoneim, "Thermal Performance of Flat Plate Solar Collector Equipped with Rectangular Cell Honeycomb," ANZSES, Kuwait, 2003.

[25] R. Winston, B. Johnston and K. Balkowski, "Development of Non-Tracking Solar Thermal Technology," 2011.

[26] R. Winston, J. C. Minano and P. G. Benitez, Nonimaging Optics, Burlington, MA: Elsevier Academic Press, 2005.

[27] C. Moe, "Radiation," May 2014. [Online]. Available: http://xycreations.com/radiation.

[28] ACT, "Solar Energy Collection and Conversion," 02 May 2015. [Online]. Available: http://www.1-act.com/markets/solar/.

[29] J. S. Coventry, "Performance of a concentrating photovoltaic/thermal solar collector," *Solar Energy,* pp. 211-222, 2005.

[30] Duratherm Fluids, "Duratherm 600," 03 May 2015. [Online]. Available: https://durathermfluids.com/pdf/productdata/heattransfer/duratherm-600-charts.pdf.

[31] R. B. Bird, W. E. Stewart and N. L. Edwin, Transport Phenomena, Second Edition, New York: John Wiley & Sons, Inc., 2007.

[32] M. F. Modest, Radiative Heat Transfer, Third Edition, New York: Academic Press, 2013.

[33] F. P. Incropera, D. P. Dewitt, T. L. Bergman and A. S. Lavine, Fundamentals of Heat and Mass Transfer, 6th ed., John Wiley & Sons, 2006.

[34] "Heat Transfer Coefficients for Submerged Coils," Apr 2013. [Online]. Available: http://www.engineeringtoolbox.com/heat-transfer-coefficients-coils-d_178.html.

[35] "Heat Loss from Open Water Tanks," March 2015. [Online]. Available: http://www.engineeringtoolbox.com/heat-loss-open-water-tanks-d_286.html.

[36] JUST, "Osmotic Potential," 20 June 2014. [Online]. Available: http://www.just.edu.jo/~plantphys/Osmotic%20potential.htm.

[37] DOE, "DOE EERE Research Reports," 20 June 2014. [Online]. Available: http://web.ornl.gov/sci/ees/etsd/btric/eere_research_reports/thermally_activated_technologies/absorption/subindex2.html.

[38] U. o. T. a. E. Paso, August 2002. [Online]. Available: http://www.usbr.gov/research/AWT/reportpdfs/report080.pdf.

[39] A. v. G. a. J. L. T. Shawn Meyer-Steele, "Seawater Reverse Osmosis Plants in the Caribbean Recover Energy and Brine and Reduce Costs," GE Power & Water, 2008.

[40] K. Fagan, "Desalinatin plants a pricey option if drought persists," 15 February 2014. [Online]. Available: http://www.sfgate.com/news/article/Desalination-plants-a-pricey-option-if-drought-5239096.php.

[41] "Boiling-point elevation," 2014. [Online]. Available: http://en.wikipedia.org/wiki/Boiling-point_elevation.

[42] T. Bott, Fouling of Heat Exchangers, Amsterdam: Elsevier, 1995.

[43] J. G. Collier and J. R. Thome, Convective Boiling and Condensation, Oxford: Clarendon Press, 1995.

[44] Purdue University, "Boiling Point Elevation," 2 February 2015. [Online]. Available: http://www.chem.purdue.edu/gchelp/solutions/eboil.html.

[45] A. P. Watkinson, "Scaling of Heat Exchanger Tubes by Calcium Carabonate," *J. Heat Transfer,* 1975.

[46] A. J. K. N. Andritsos, "Calcium carbonate scaling in a plate heat exchanger in the presence of particles," *International Journal of Heat and Mass Transfer,* p. 4613–4627, 2003.

[47] D. Hasson, M. Avriel, W. Resnick, T. Rozenman and S. Windreich, "Mechanism of Calcium Carbonate Scale Depositon on Heat-Transfer Surfaces," *Ind. Eng. Chem. Fundamen.,* p. 59–65, 1968.

[48] C. Fritzmann, J. Lowenberg, T. Wintgens and T. Melin, "State-of-the-art of reverse osmosis desalination," *Desalination,* pp. 1-76, 2007.

[49] Lenntech, "Reverse Osmosis Pretreatment," 02 May 2015. [Online]. Available: http://www.lenntech.com/ro/ro-pretreatment.htm.

Appendix

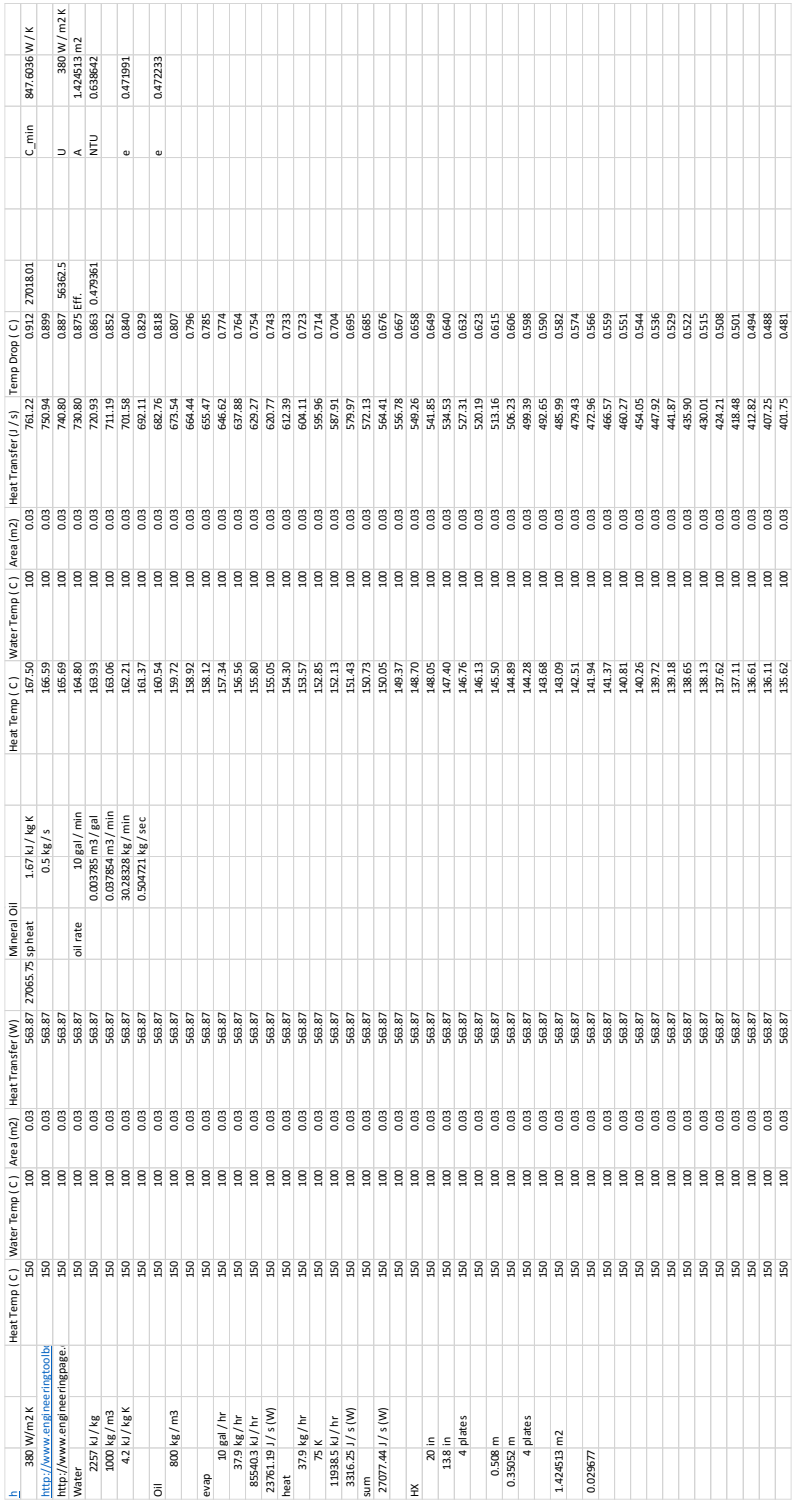

h		Heat Temp (C)	Water Temp (C)	Area (m2)	Heat Transfer (W)		Mineral Oil		Heat Temp (C)	Water Temp (C)	Area (m2)	Heat Transfer (J / s)	Temp Drop (C)			
380 W/m2 K		150	100	0.03	563.87	27065.75	sp heat	1.67 kJ / kg K	167.50	100	0.03	761.22	0.912	27018.01	C_min	847.6036 W / K
http://www.engineeringtoolbo		150	100	0.03	563.87			0.5 kg / s	166.59	100	0.03	750.94	0.899			
http://www.engineeringpage.		150	100	0.03	563.87				165.69	100	0.03	740.80	0.887	56362.5	U	380 W / m2 K
Water		150	100	0.03	563.87		oil rate	10 gal / min	164.80	100	0.03	730.80	0.875	Eff.	A	1.424513 m2
2257 kJ / kg		150	100	0.03	563.87			0.003785 m3 / gal	163.93	100	0.03	720.93	0.863	0.479361	NTU	0.638642
1000 kg / m3		150	100	0.03	563.87			0.037854 m3 / min	163.06	100	0.03	711.19	0.852			
4.2 kJ / kg K		150	100	0.03	563.87			30.28328 kg / min	162.21	100	0.03	701.58	0.840		e	0.471991
		150	100	0.03	563.87			0.504721 kg / sec	161.37	100	0.03	692.11	0.829			
Oil		150	100	0.03	563.87				160.54	100	0.03	682.76	0.818		e	0.472233
800 kg / m3		150	100	0.03	563.87				159.72	100	0.03	673.54	0.807			
		150	100	0.03	563.87				158.92	100	0.03	664.44	0.796			
evap		150	100	0.03	563.87				158.12	100	0.03	655.47	0.785			
10 gal / hr		150	100	0.03	563.87				157.34	100	0.03	646.62	0.774			
37.9 kg / hr		150	100	0.03	563.87				156.56	100	0.03	637.88	0.764			
855403 kJ / hr		150	100	0.03	563.87				155.80	100	0.03	629.27	0.754			
23761.19 J / s (W)		150	100	0.03	563.87				155.05	100	0.03	620.77	0.743			
heat		150	100	0.03	563.87				154.30	100	0.03	612.39	0.733			
37.9 kg / hr		150	100	0.03	563.87				153.57	100	0.03	604.11	0.723			
75 K		150	100	0.03	563.87				152.85	100	0.03	595.96	0.714			
119385 kJ / hr		150	100	0.03	563.87				152.13	100	0.03	587.91	0.704			
3316.25 J / s (W)		150	100	0.03	563.87				151.43	100	0.03	579.97	0.695			
sum		150	100	0.03	563.87				150.73	100	0.03	572.13	0.685			
27077.44 J / s (W)		150	100	0.03	563.87				150.05	100	0.03	564.41	0.676			
		150	100	0.03	563.87				149.37	100	0.03	556.78	0.667			
HX		150	100	0.03	563.87				148.70	100	0.03	549.26	0.658			
20 in		150	100	0.03	563.87				148.05	100	0.03	541.85	0.649			
13.8 in		150	100	0.03	563.87				147.40	100	0.03	534.53	0.640			
4 plates		150	100	0.03	563.87				146.76	100	0.03	527.31	0.632			
		150	100	0.03	563.87				146.13	100	0.03	520.19	0.623			
0.508 m		150	100	0.03	563.87				145.50	100	0.03	513.16	0.615			
0.35052 m		150	100	0.03	563.87				144.89	100	0.03	506.23	0.606			
4 plates		150	100	0.03	563.87				144.28	100	0.03	499.39	0.598			
		150	100	0.03	563.87				143.68	100	0.03	492.65	0.590			
1.424513 m2		150	100	0.03	563.87				143.09	100	0.03	485.99	0.582			
		150	100	0.03	563.87				142.51	100	0.03	479.43	0.574			
0.029677		150	100	0.03	563.87				141.94	100	0.03	472.96	0.566			
		150	100	0.03	563.87				141.37	100	0.03	466.57	0.559			
		150	100	0.03	563.87				140.81	100	0.03	460.27	0.551			
		150	100	0.03	563.87				140.26	100	0.03	454.05	0.544			
		150	100	0.03	563.87				139.72	100	0.03	447.92	0.536			
		150	100	0.03	563.87				139.18	100	0.03	441.87	0.529			
		150	100	0.03	563.87				138.65	100	0.03	435.90	0.522			
		150	100	0.03	563.87				138.13	100	0.03	430.01	0.515			
		150	100	0.03	563.87				137.62	100	0.03	424.21	0.508			
		150	100	0.03	563.87				137.11	100	0.03	418.48	0.501			
		150	100	0.03	563.87				136.61	100	0.03	412.82	0.494			
		150	100	0.03	563.87				136.11	100	0.03	407.25	0.488			
		150	100	0.03	563.87				135.62	100	0.03	401.75	0.481			

Figure 26: Evaporator Heat Exchanger Breakdown Configured with Steam and Thermal Oil

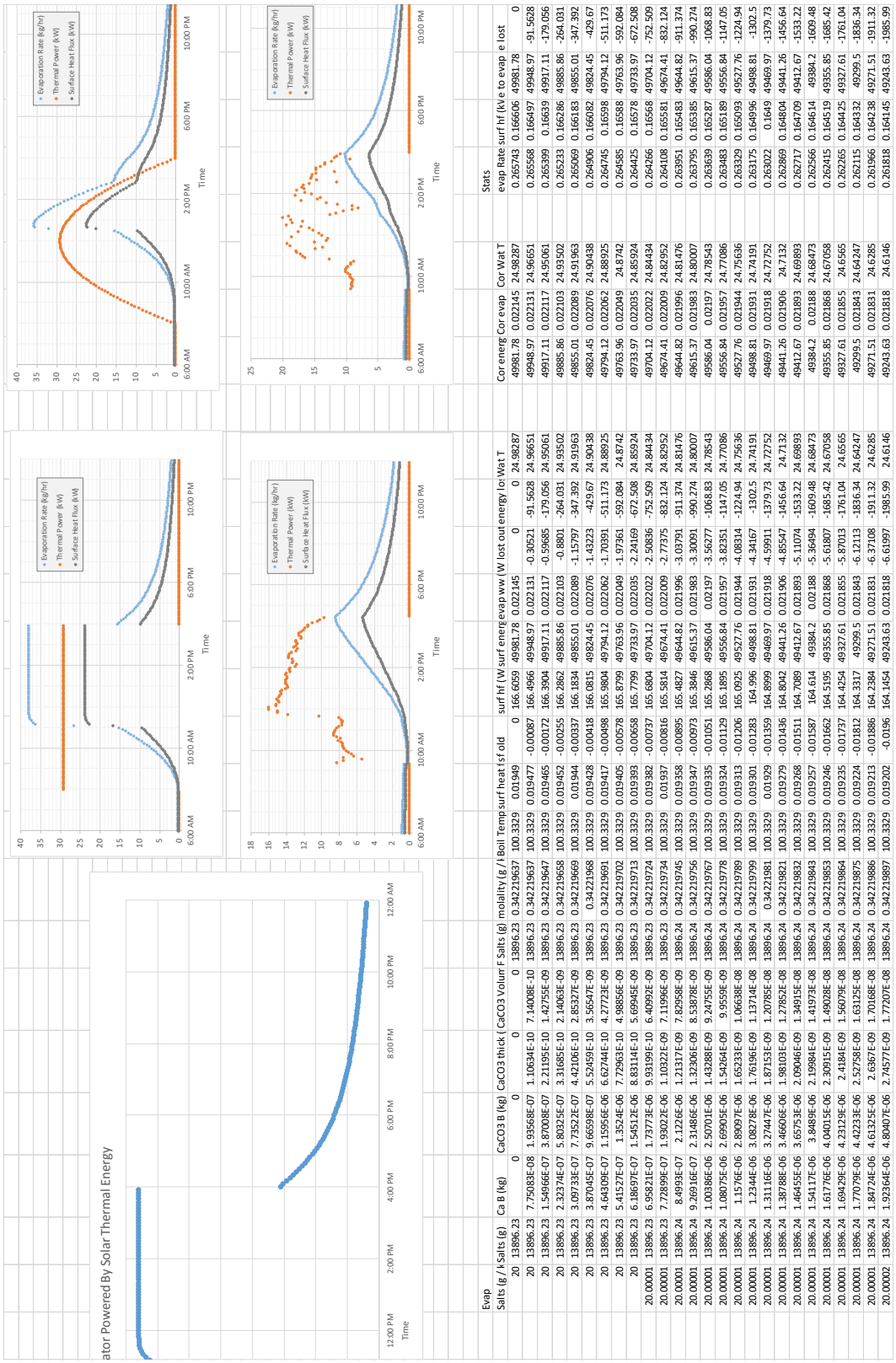

Evap Salts (g)	Ca B (kg)	CaCO3 B (kg)	CaCO3 thick (m)	CaCO3 Volume (m3)	Salts (g)	molality (g / kg)	Boil Temp	surf heat loss (W)	surf hf (W/m2)	surf energy (W)	evap ww (W)	lost out energy (W)	Wat T	Cor energy (W)	Cor evap (kg/hr)	Cor Wat T	Stats evap Rate (kg/hr)	surf hf (kW/m2)	evap energy (kW)	lost (W)
20	13896.23	0	0	0	13896.23	0.342219637	100.3329	0.01949	0	166.6059	49981.78	0.022145	0	24.98287	49981.78	0.022145	24.98287	0.265743	0.166606	49981.78	0
20	13896.23	7.75083E-08	1.93568E-07	1.10634E-10	13896.23	0.342219637	100.3329	0.019477	-0.00087	166.4966	49948.97	0.022131	-0.30521	-91.5628	49948.97	0.022131	24.96651	0.265568	0.166497	49948.97	-91.5628
20	13896.23	1.54966E-07	3.87008E-07	2.21195E-10	1.42755E-09	13896.23	0.342219647	100.3329	0.019465	-0.00172	166.3904	49917.11	0.022117	-0.59685	-179.056	24.95061	49917.11	0.022117	24.95061	0.265399	0.16639	49917.11	-179.056
20	13896.23	2.32374E-07	5.80325E-07	3.31685E-10	2.14063E-09	13896.23	0.342219658	100.3329	0.019452	-0.00255	166.2862	49885.86	0.022103	-0.8801	-264.031	24.93502	49885.86	0.022103	24.93502	0.265233	0.166286	49885.86	-264.031
20	13896.23	3.09733E-07	7.73522E-07	4.42106E-10	2.85327E-09	13896.23	0.342219669	100.3329	0.01944	-0.00337	166.1834	49855.01	0.022089	-1.15797	-347.392	24.91963	49855.01	0.022089	24.91963	0.265069	0.166183	49855.01	-347.392
20	13896.23	3.87045E-07	9.66598E-07	5.52459E-10	3.56547E-09	13896.23	0.34221968	100.3329	0.019428	-0.00418	166.0815	49824.45	0.022076	-1.43223	-429.67	24.90438	49824.45	0.022076	24.90438	0.264906	0.166082	49824.45	-429.67
20	13896.23	4.64309E-07	1.15956E-06	6.62744E-10	4.27723E-09	13896.23	0.342219691	100.3329	0.019417	-0.00498	165.9804	49794.12	0.022062	-1.70391	-511.173	24.88925	49794.12	0.022062	24.88925	0.264745	0.16598	49794.12	-511.173
20	13896.23	5.41527E-07	1.3524E-06	7.72963E-10	4.98856E-09	13896.23	0.342219702	100.3329	0.019405	-0.00578	165.8799	49763.96	0.022049	-1.97361	-592.084	24.8742	49763.96	0.022049	24.8742	0.264585	0.16588	49763.96	-592.084
20	13896.23	6.18697E-07	1.54512E-06	8.83114E-10	5.69945E-09	13896.23	0.342219713	100.3329	0.019393	-0.00658	165.7799	49733.97	0.022035	-2.24169	-672.508	24.85924	49733.97	0.022035	24.85924	0.264425	0.16578	49733.97	-672.508
20.00001	13896.23	6.95821E-07	1.73773E-06	9.93199E-10	6.40992E-09	13896.23	0.342219724	100.3329	0.019382	-0.00737	165.6804	49704.12	0.022022	-2.50836	-752.509	24.84434	49704.12	0.022022	24.84434	0.264266	0.16568	49704.12	-752.509
20.00001	13896.23	7.72899E-07	1.93022E-06	1.10322E-09	7.11996E-09	13896.23	0.342219734	100.3329	0.01937	-0.00816	165.5814	49674.41	0.022009	-2.77375	-832.124	24.82952	49674.41	0.022009	24.82952	0.264108	0.165581	49674.41	-832.124
20.00001	13896.24	8.4993E-07	2.1226E-06	1.21317E-09	7.82958E-09	13896.24	0.342219745	100.3329	0.019358	-0.00895	165.4827	49644.82	0.021996	-3.03791	-911.374	24.81476	49644.82	0.021996	24.81476	0.263951	0.165483	49644.82	-911.374
20.00001	13896.24	9.26916E-07	2.31486E-06	1.32306E-09	8.53878E-09	13896.24	0.342219756	100.3329	0.019347	-0.00973	165.3846	49615.37	0.021983	-3.30091	-990.274	24.80007	49615.37	0.021983	24.80007	0.263795	0.165385	49615.37	-990.274
20.00001	13896.24	1.00386E-06	2.50701E-06	1.43288E-09	9.24755E-09	13896.24	0.342219767	100.3329	0.019335	-0.01051	165.2868	49586.04	0.02197	-3.56277	-1068.83	24.78543	49586.04	0.02197	24.78543	0.263639	0.165287	49586.04	-1068.83
20.00001	13896.24	1.08075E-06	2.69905E-06	1.54264E-09	9.9559E-09	13896.24	0.342219778	100.3329	0.019324	-0.01129	165.1895	49556.84	0.021957	-3.82351	-1147.05	24.77086	49556.84	0.021957	24.77086	0.263483	0.165189	49556.84	-1147.05
20.00001	13896.24	1.1576E-06	2.89097E-06	1.65233E-09	1.06638E-08	13896.24	0.342219789	100.3329	0.019313	-0.01206	165.0925	49527.76	0.021944	-4.08314	-1224.94	24.75636	49527.76	0.021944	24.75636	0.263329	0.165093	49527.76	-1224.94
20.00001	13896.24	1.2344E-06	3.08278E-06	1.76196E-09	1.13714E-08	13896.24	0.342219799	100.3329	0.019301	-0.01283	164.996	49498.81	0.021931	-4.34167	-1302.5	24.74191	49498.81	0.021931	24.74191	0.263175	0.164996	49498.81	-1302.5
20.00001	13896.24	1.31116E-06	3.27447E-06	1.87153E-09	1.20785E-08	13896.24	0.34221981	100.3329	0.01929	-0.01359	164.8999	49469.97	0.021918	-4.59911	-1379.73	24.72752	49469.97	0.021918	24.72752	0.263022	0.1649	49469.97	-1379.73
20.00001	13896.24	1.38788E-06	3.46606E-06	1.98103E-09	1.27852E-08	13896.24	0.342219821	100.3329	0.019279	-0.01436	164.8042	49441.26	0.021906	-4.85547	-1456.64	24.7132	49441.26	0.021906	24.7132	0.262869	0.164804	49441.26	-1456.64
20.00001	13896.24	1.46455E-06	3.65753E-06	2.09046E-09	1.34915E-08	13896.24	0.342219832	100.3329	0.019268	-0.01511	164.7089	49412.67	0.021893	-5.11074	-1533.22	24.69893	49412.67	0.021893	24.69893	0.262717	0.164709	49412.67	-1533.22
20.00001	13896.24	1.54117E-06	3.84899E-06	2.19984E-09	1.41973E-08	13896.24	0.342219843	100.3329	0.019257	-0.01587	164.614	49384.2	0.02188	-5.36494	-1609.48	24.68473	49384.2	0.02188	24.68473	0.262566	0.164614	49384.2	-1609.48
20.00001	13896.24	1.61776E-06	4.04015E-06	2.30915E-09	1.49028E-08	13896.24	0.342219853	100.3329	0.019246	-0.01662	164.5195	49355.85	0.021868	-5.61807	-1685.42	24.67058	49355.85	0.021868	24.67058	0.262415	0.164519	49355.85	-1685.42
20.00001	13896.24	1.69429E-06	4.23129E-06	2.4184E-09	1.56079E-08	13896.24	0.342219864	100.3329	0.019235	-0.01737	164.4254	49327.61	0.021855	-5.87013	-1761.04	24.6565	49327.61	0.021855	24.6565	0.262265	0.164425	49327.61	-1761.04
20.00001	13896.24	1.77079E-06	4.42233E-06	2.52758E-09	1.63125E-08	13896.24	0.342219875	100.3329	0.019224	-0.01812	164.3317	49299.5	0.021843	-6.12113	-1836.34	24.64247	49299.5	0.021843	24.64247	0.262115	0.164332	49299.5	-1836.34
20.00001	13896.24	1.84724E-06	4.61325E-06	2.6367E-09	1.70168E-08	13896.24	0.342219886	100.3329	0.019213	-0.01886	164.2384	49271.51	0.021831	-6.37108	-1911.32	24.6285	49271.51	0.021831	24.6285	0.261966	0.164238	49271.51	-1911.32
20.00002	13896.24	1.92364E-06	4.80407E-06	2.74577E-09	1.77207E-08	13896.24	0.342219897	100.3329	0.019202	-0.0196	164.1454	49243.63	0.021818	-6.61997	-1985.99	24.6146	49243.63	0.021818	24.6146	0.261818	0.164145	49243.63	-1985.99

Figure 27: Simulation clip, right

Figure 28: Simulation clip, center

Water					0.8128	m						Warm up time			Rough Check				heat loss from water due to evaporation (http://www.engin		
2257	kJ / kg				0.635	m						694.8115	kg		37.25083	kg / hr			Water Temp	Heat Loss (W / cm2)	
1000	kg / m3				1.3462	m						75	K		81.95182	lb / hr			0	0	
4.2	kJ / kg K				0.0254	m					heat neec	218865.6	kJ		8.3	lb / gal			32.222	0.02512	
												7508.255	s		9.873713	gal / hr			37.778	0.05024	
Oil				CaCO3			Ca					2.085626	hr						43.334	0.07536	
800	kg / m3			100.09	g / mol		40.078	g / mol											48.89	0.11304	
1.67	kJ / kg K			2.711	g / cm3		0.175	g Ca / g salt											54.446	0.15072	
0.5	kg / s			271.1	kg / m3														60.002	0.20724	
0.162	W / m K (Thermal cond.)			0.4 - 2.6	W / m K		Co Br												65.558	0.27004	
				0.8	W / m K (est)		60	W / m K (est)											71.114	0.3454	
NaCl																			76.67	0.43332	
58.4	g / mol																		82.226	0.54636	
																			87.782	0.67824	
Configuration																			93.338	0.84152	
Loop					Evaporator				Evaporator HX				Tank						98.894	1.01736	
Power:	29.15	kW			Water Dim				20	in			Conc.	20	g / kg_sol				105	1.3	
	29.15	kJ / s			h	32	in		13.8	in			NaCl	58.442	g / mol						
	104940	kJ / hr			w	25	in		4	plates			I (van't Ho	1.9			Results				
	8	hrs			l	53	in						K_b	0.512			Evap Rate	0.27	kg / hr		
oil mass	200	kg			Phys Dim				0.508	m							Oil T	58.48	C		
loop ins	0.045	W / m K			h	1.83	m		0.35052	m							Wat T	25.21	C		
loop ins tl	0.04	m			w	0.74	m		0.002	m			Environment				Wat Pow	26.61	kW		
loop dia	0.1	m			l	1.43	m		4	plates			Temp	25	C			95809.13	kJ / hr		
loop len	60	m			wall thick	1	in														
loop area	18.84956	m2			evap ins	0.045	W / m K		2.34E-05	K / W (Co Resistivity)			cevap @1(	4	W / cm2		Evaporate	248.3414	kg		
loop hx t	21.20575	W / K							0.021666	K / W (Static Oil Resistivity)											
					volume	0.694812	m3										E Used	839520	kJ		
					surface ar	10.0586	m2		1.424513	m2							E Water	560506.6	kJ		
					wall hx t	17.82035	W / K		541.315	W / K			brine suface area					0.667651	eff.		
dt	ts				heat x h	380	W / m2 K		0.001847	K / W (Tot Resistivity)			0.854837	m2				5.850242	eff. Hr		
5	0																				
		Loop									Evaporator							HX			
time		power	Oil T in	Oil T out	W lost out	W lost in	J gain	T gain			Oil T in	Oil T out	Wat In	Wat Rem	Wat T In	Wat T	Vap T Out	Sections	CaCO3 Res. (K	Tot Res. (K/W	Conductance (W/K)
0	12:00 AM	0	25	25	0	0	0	0			25	25	0	694.8115	25	25	25	10	0	0.001847353	541.315
5	12:05 AM	0	25	25	0	-0.11826	-2059.995	-0.00617			25	24.99163	0.022145	694.7894	25	24.98287	24.98287	10	9.70802E-11	0.001847353	541.315
10	12:10 AM	0	24.99383	24.99383	-0.0436	-0.27549	-3253.868	-0.00974			24.99388	24.98051	0.022131	694.7894	25	24.96651	24.96651	10	1.94097E-10	0.001847353	541.315
15	12:15 AM	0	24.98409	24.98409	-0.11246	-0.4551	-3942.17	-0.0118			24.98422	24.96781	0.022117	694.7894	25	24.95061	24.95061	10	2.91051E-10	0.001847353	541.315
20	12:20 AM	0	24.97229	24.97229	-0.19589	-0.64741	-4335.377	-0.01298			24.97252	24.95421	0.022103	694.7894	25	24.93502	24.93502	10	3.87945E-10	0.001847353	541.3149
25	12:25 AM	0	24.95931	24.95931	-0.28764	-0.84676	-4556.355	-0.01364			24.95965	24.9401	0.022089	694.7894	25	24.91963	24.91963	10	4.84779E-10	0.001847354	541.3149
30	12:30 AM	0	24.94567	24.94567	-0.38407	-1.04985	-4676.828	-0.014			24.94613	24.92574	0.022076	694.7894	25	24.90438	24.90438	10	5.81553E-10	0.001847354	541.3149
35	12:35 AM	0	24.93166	24.93166	-0.48305	-1.25477	-4738.667	-0.01419			24.93224	24.91124	0.022062	694.7895	25	24.88925	24.88925	10	6.78269E-10	0.001847354	541.3148
40	12:40 AM	0	24.91748	24.91748	-0.58333	-1.46038	-4766.313	-0.01427			24.91817	24.8967	0.022049	694.7895	25	24.87421	24.87421	10	7.74926E-10	0.001847354	541.3148
45	12:45 AM	0	24.9032	24.9032	-0.6842	-1.66604	-4774.034	-0.01429			24.90402	24.88215	0.022035	694.7895	25	24.85924	24.85924	10	8.71525E-10	0.001847354	541.3148
50	12:50 AM	0	24.88891	24.88891	-0.78524	-1.87137	-4770.159	-0.01428			24.88985	24.86763	0.022022	694.7895	25	24.84435	24.84435	10	9.68066E-10	0.001847354	541.3148
55	12:55 AM	0	24.87463	24.87463	-0.88619	-2.07614	-4759.551	-0.01425			24.87569	24.85314	0.022009	694.7895	25	24.82953	24.82953	10	1.06455E-09	0.001847354	541.3147
60	1:00 AM	0	24.86038	24.86038	-0.98692	-2.28024	-4745.047	-0.01421			24.86156	24.83871	0.021996	694.7895	25	24.81477	24.81477	10	1.16097E-09	0.001847354	541.3147
65	1:05 AM	0	24.84617	24.84617	-1.08734	-2.48358	-4728.304	-0.01416			24.84747	24.82432	0.021983	694.7895	25	24.80007	24.80007	10	1.25734E-09	0.001847354	541.3147
70	1:10 AM	0	24.83202	24.83202	-1.18741	-2.68613	-4710.288	-0.0141			24.83344	24.81	0.02197	694.7895	25	24.78544	24.78544	10	1.35365E-09	0.001847354	541.3146
75	1:15 AM	0	24.81791	24.81791	-1.28709	-2.88786	-4691.565	-0.01405			24.81945	24.79573	0.021957	694.7896	25	24.77087	24.77087	10	1.44991E-09	0.001847354	541.3146
80	1:20 AM	0	24.80387	24.80387	-1.38638	-3.08876	-4672.463	-0.01399			24.80553	24.78152	0.021944	694.7896	25	24.75636	24.75636	10	1.54611E-09	0.001847355	541.3146
85	1:25 AM	0	24.78988	24.78988	-1.48527	-3.28883	-4653.175	-0.01393			24.79166	24.76736	0.021931	694.7896	25	24.74192	24.74192	10	1.64225E-09	0.001847355	541.3146
90	1:30 AM	0	24.77595	24.77595	-1.58375	-3.48806	-4633.811	-0.01387			24.77784	24.75327	0.021918	694.7896	25	24.72753	24.72753	10	1.73834E-09	0.001847355	541.3145
95	1:35 AM	0	24.76207	24.76207	-1.68181	-3.68646	-4614.439	-0.01382			24.76409	24.73924	0.021906	694.7896	25	24.71321	24.71321	10	1.83437E-09	0.001847355	541.3145
100	1:40 AM	0	24.74826	24.74826	-1.77947	-3.88403	-4595.095	-0.01376			24.75039	24.72526	0.021893	694.7896	25	24.69894	24.69894	10	1.93034E-09	0.001847355	541.3145
105	1:45 AM	0	24.7345	24.7345	-1.87672	-4.08077	-4575.801	-0.0137			24.73675	24.71134	0.02188	694.7896	25	24.68474	24.68474	10	2.02626E-09	0.001847355	541.3145
110	1:50 AM	0	24.7208	24.7208	-1.97356	-4.27668	-4556.571	-0.01364			24.72316	24.69749	0.021868	694.7896	25	24.67059	24.67059	10	2.12212E-09	0.001847355	541.3144
115	1:55 AM	0	24.70716	24.70716	-2.06999	-4.47177	-4537.411	-0.01359			24.70964	24.68369	0.021855	694.7897	25	24.65651	24.65651	10	2.21793E-09	0.001847355	541.3144
120	2:00 AM	0	24.69357	24.69357	-2.16602	-4.66603	-4518.326	-0.01353			24.69617	24.66995	0.021843	694.7897	25	24.64248	24.64248	10	2.31369E-09	0.001847355	541.3144
125	2:05 AM	0	24.68004	24.68004	-2.26164	-4.85948	-4499.318	-0.01347			24.68275	24.65626	0.021831	694.7897	25	24.62852	24.62852	10	2.40939E-09	0.001847355	541.3143

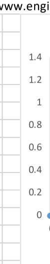

Figure 29: Simulation clip, left